# A bivalent EBV vaccine induces neutralizing antibodies that block B and epithelial cell infection and confer immunity in humanized mice

Chih-Jen Wei[1,2*], Wei Bu[3*], Laura A. Nguyen[1*§], Joseph D. Batchelor[4], JungHyun Kim[3], Stefania Pittaluga[5], James R. Fuller[4§], Hanh Nguyen[3], Te-Hui Chou[1,2], Jeffrey I. Cohen[3†], Gary J. Nabel[1,2†]

[1]Sanofi,
640 Memorial Dr., Cambridge, MA.01239

[2]ModeX Therapeutics Inc.
22 Strathmore Rd., Natick, MA 07160

[3]Laboratory of Infectious Diseases, National Institute of Allergy and Infectious Diseases, National Institute of Health.
50 South Dr., Bethesda, MD. 20892

[4]Integrated Drug Discovery, Sanofi,
Waltham, MA.02451

[5]Laboratory of Pathology, Center for Cancer Research, National Cancer Institute, National Institutes of Health, Bethesda, MD 20892

[*] These authors contributed equally to this work.

[†] To whom correspondence should be addressed: Gary J. Nabel (gary.nabel@modextx.com); Jeffrey I. Cohen (jcohen@niaid.nih.gov)

[§] Current address: Omega Therapeutics, Cambridge, MA (L. Nguyen); Department of Biochemistry and Molecular Biology, University of Chicago, Chicago, IL (J. R. Fuller)

**One sentence summary:** A bivalent gp350 and gH/gL/gp42 nanoparticle vaccine elicits neutralizing antibodies that protect against EBV infection and EBV lymphoma *in vivo.*

## ABSTRACT

**Epstein Barr virus (EBV) is the major cause of infectious mononucleosis and is associated with several human cancers. Despite its prevalence and major impact on human health, there are currently no specific vaccines or treatments. Four viral glycoproteins, gp 350 and gH/gL/gp42 mediate entry into the major sites of viral replication, B cells and epithelial cells. Here, we designed a nanoparticle vaccine displaying these proteins and show that it elicits potent neutralizing antibodies that protect against infection *in vivo*. Based on structural analyses, we designed single chain gH/gL and gH/gL/gp42 proteins that were each fused to bacterial ferritin to form a self-assembling nanoparticles. X-ray crystallographic analysis revealed that single chain gH/gL and gH/gL/gp42 adopted a similar conformation to the wild type proteins, and the protein spikes were observed by electron microscopy. Single chain gH/gL or gH/gL/gp42 nanoparticle vaccines were constructed to ensure product homogeneity needed for clinical development. These vaccines elicited neutralizing antibodies in mice, ferrets, and non-human primates that inhibited EBV entry into both B cells and epithelial cells. When mixed with a previously reported gp350 nanoparticle vaccine, gp350D$_{123}$, no immune competition was observed. To confirm its efficacy in vivo, humanized mice were challenged with EBV after passive transfer of IgG from mice vaccinated with control, gH/gL/gp42+gp350D$_{123}$ or gH/gL+gp350D$_{123}$ nanoparticles. While all control animals (6/6) were infected, only one mouse in each vaccine group that received immune IgG had transient low level viremia (1/6). Furthermore, no EBV lymphomas were detected in immune animals in contrast to non-immune controls. This bivalent EBV nanoparticle vaccine represents a promising candidate to prevent EBV infection and EBV-related malignancies in humans.**

## INTRODUCTION

Over 95% of adults worldwide are infected with Epstein-Barr virus (EBV), the primary agent for infectious mononucleosis (IM) (*1*). EBV was discovered in the 1960s and was the first human virus associated with cancer; EBV has since been associated with malignancies such as nasopharyngeal carcinoma, Hodgkin's lymphoma, non-Hodgkin's lymphoma, Burkitt's lymphoma, NK/T cell lymphomas, peripheral T-cell lymphomas and gastric cancer (*1, 2*). Each year, more than 200,000 cases of cancer are associated with EBV infection, resulting in ~140,000 deaths (*2*). EBV is also the main cause of lymphoproliferative disease in patients with immunodeficiencies. Nearly all post-transplant lymphoproliferative disorder (PTLD) in the first year after is caused by EBV (*3*).

There is currently no therapy to effectively treat EBV infection, and there is no vaccine to prevent EBV infection. Prior vaccine development attempts mainly focused on one of the viral envelope glycoproteins gp350 as it is the most abundant surface protein and is the major target of neutralizing antibodies (*4*). gp350 mediates viral entry to B cells by engaging complement receptor 2 (CR2/CD21) (*5*). Other viral surface glycoproteins, namely gH, gL, gB, gp42 and BMRF2 also play a role in EBV infection and are also targets of neutralizing antibodies. gp42 binds to human leukocyte antigen (HLA) class II and together with gH/gL heterodimer and gB forms a complex that promotes EBV entry to B cells (*6*). Infection of EBV to epithelial cells is initiated by the engagement of BMRF2 and gH/gL complex with integrin receptors and ephrin receptor A2 (*7-9*). A prototype gp350 vaccine reduced the incidence of IM by 78%, but did not prevent infection in a phase II clinical trial (*10*). Other gp350-based vaccines have also shown protective efficacy in relevant nonhuman primate models (*7, 11, 12*). Recombinant gH/gL complex or gB have also been shown to induce neutralizing antibody responses in rabbits (*13*). We have previously shown that

a nanoparticle (NP)-based gp350 vaccine elicited protective immunity (*14*), and gH/gL and gH/gL/g42 NP vaccines induced potent neutralizing antibodies that inhibit EBV entry in both B cells and epithelial cells (*15*). In this study, we optimized the consistency of gH/gL and gH/gL/gp42 that could reduce the heterogeneity of these heteromeric proteins by generating a single chain polypeptide based on structural biology. This approach not only preserved the presentation of these antigens but also ensured that the gH/gL and gp42 heteromers were uniformly assembled to improve product consistency required for clinical grade vaccines. Here, we have evaluated the structure, immunogenicity and protection of single chain gH/gL-NP or single chain gH/gL/gp42-NP together with gp350-NP in relevant animal models.

## RESULTS

### Design and characterization of single chain gH/gL and gH/gL/gp42 nanoparticles

When co-transfection of plasmids is used to generate multimeric complexes (*15*), there is potential inconsistency in the product if the appropriate stoichiometry is not achieved. To address this concern, we generated single chain gH/gL or gH/gL/gp42 complexes using structural data to fuse the ectodomains with flexible linkers (Fig. 1A). Fusion to specific sites on ferritin (*14*) facilitated the formation of self-assembling nanoparticles (NP). The gH/gL and gH/gL/gp42 fusion proteins migrated as a single band on SDS-PAGE gel (Fig. S1). Crystal structures of single chain gH/gL and single chain gH/gL/gp42 were determined (Fig. 1B; Supplemental Table 1). Each structure superimposed on previously published heterodimeric gH/gL (PDB 3PHF) and heterotrimeric gH/gL/gp42 (PDB 5T1D) complex structures, respectively, demonstrating that single chain gH/gL and single chain gH/gL/gp42 adopt native conformations resembling the wild-type complexes (Fig. 1B). Both gH/gL-NP and gH/gL/gp42-NP could be purified by ion exchange

and size-exclusion chromatography (Fig. 1C, left), and dynamic light scattering analysis documented the expected particle radius of 20.7 nm and 24.8 nm for single chain gH/gL-NP and single chain gH/gL/gp42-NP, respectively (Fig 1C, right). The single chain gH/gL-NP and single chain gH/gL/gp42-NP were also visualized by transmission electron microscopy, showing visible spikes protruding from the ferritin core, consistent with the expected structure and stoichiometry (Fig. 1D, left and right panels respectively).

**Immunogenicity of single chain gH/gL-NP or gH/gL/gp42-NP in mice**

The immunogenicity of single chain gH/gL-NP was first evaluated in mice with or without AF03, a squalene-based oil-in-water emulsion adjuvant previously used in a pandemic influenza vaccine (*16*). The anti-gH/gL antibody titer was significantly higher in the adjuvanted group after each immunization (Supplemental Fig. 2, $p<0.0001$). All subsequent animal studies were therefore carried out in the presence of AF03 adjuvant. Single chain gH/gL-NP elicited a robust antibody response against the gH/gL complex and when used together with the previously described gp350$D_{123}$-NP (*14*), no immune competition was seen (Supplemental Fig. 3). Similar results were observed when gp42 was included to generate a single chain gH/gL/gp42-NP that induced antibodies against both gH/gL and gp42 after immunization (Supplemental Fig. 4A). Again, no immune competition was observed when mice were given a bivalent single chain-gH/gL/gp42-NP and gp350$D_{123}$-NP vaccine as the antibodies titers against each individual antigen remained at the similar levels (Supplemental Fig. 4B). The neutralizing activity of sera from animals immunized with single chain gH/gL-NP and single chain gH/gL/gp42-NP were evaluated in both B cells and epithelial cells (Fig 2). Single chain gH/gL-NP, gH/gL/gp42-NP and gp350$D_{123}$-NP all elicited potent neutralizing antibodies that blocked virus entry to B cells, and the neutralizing $IC_{50}$ titers remained at similar or higher levels when single chain gH/gL-NP or single chain gH/gL/gp42-NP

was mixed with gp350D$_{123}$-NP in a bivalent vaccine (Fig. 2A, 2B, left, $p<0.05$ compared to control). Virus neutralization in epithelial cells was also evident in mice that received single chain gH/gL-NP and single chain gH/gL/gp42-NP while gp350D$_{123}$-NP antiserum had minimum effect in blocking EBV infection in epithelial cells, consistent with our previous report (*15*) (Fig. 2A, right, $p<0.05$ compared to control). Again, bivalent single chain gH/gL-NP+gp350D$_{123}$-NP or single chain gH/gL/gp42-NP+gp350D$_{123}$-NP induced similar neutralizing antibody titers as the monovalent single chain gH/gL-NP and single chain gH/gL/gp42-NP, respectively (Fig. 2A, 2B, right, $p<0.05$ compared to control).

**Bivalent single chain gH/gL-NP+gp350D$_{123}$-NP or single chain gH/gL/gp42-NP+gp350D$_{123}$-NP elicited neutralizing antibodies in ferrets and non-human primates**

We next evaluated the immunogenicity of bivalent single chain gH/gL-NP+gp350D$_{123}$-NP and single chain gH/gL/gp42-NP+gp350D$_{123}$-NP in EBV-naïve ferrets. Non-immune ferrets were immunized with 2 doses of single chain gH/gL-NP+gp350D$_{123}$-NP or single chain gH/gL/gp42-NP+gp350D$_{123}$-NP at weeks 0 and 4. Immune sera from ferrets receiving single chain gH/gL/gp42-NP+gp350D$_{123}$-NP elicited more potent neutralizing antibodies that inhibit virus entry to B cells than animals immunized with single chain gH/gL-NP+gp350D$_{123}$-NP (Fig 3A, left, $p<0.05$ compared to pre-immune sera). In epithelial cells, both single chain gH/gL-NP+gp350D$_{123}$-NP and single chain gH/gL/gp42-NP+gp350D$_{123}$-NP anti-sera showed high titers of antibodies that neutralized EBV infection (Fig 3A, right, $p<0.05$ compared to pre-immune sera). These findings were confirmed by measuring ELISA binding of antibodies to each component elicited by each bivalent vaccine (Supplemental Fig. 5, $^{**}p<0.0001$ or $^{*}p<0.05$ respectively compared to pre-immune sera). Background reactivity observed in pre-immune ferret sera likely represented non-specific binding of the secondary anti-ferret antibody as it was not observed in

the neutralization assay. Despite this background, antibody levels increased 9-400-fold after immunization.

A high percentage of rhesus macaques are infected naturally during infancy with rhesus lymphocryptovirus (rhLCV), a herpesvirus closely related and immunologically cross-reactive with EBV (*17*). To determine whether vaccination could boost pre-existing immune responses, we immunized rhesus macaques (*Macaca mulatta*) with single chain gH/gL-NP+gp350$D_{123}$-NP or single chain gH/gL/gp42-NP+gp350$D_{123}$-NP to model immune responses in humans. After the third immunization, serum neutralization titers in animals receiving single chain gH/gL-NP+gp350$D_{123}$-NP or single chain gH/gL/gp42-NP+gp350$D_{123}$-NP were substantially elevated compared to the pre-immune sera (Fig 3B, left; 10,000-fold for single chain gH/gL-NP+gp350$D_{123}$-NP and >2,000-fold for single chain gH/gL/gp42-NP+gp350$D_{123}$-NP, * $p< 0.05$ compared to pre-immune sera). As expected, substantial reactivity was observed in pre-immune sera (Supplemental Fig. 6, top and bottom left), likely due to the high amino acid sequence identity between EBV and rhLCV gH (85.4%), gL (81.8%) and gp42 (88%) (*17*). Similar to the pre-existing anti-gH/gL and anti-gH/gL/gp42 binding antibodies, neutralizing activity was observed in epithelial cells with the pre-immune monkey sera. Nonetheless, the neutralizing antibody titers increased by more than 20- and ~7-fold after the third immunization with single chain gH/gL-NP+gp350$D_{123}$-NP and single chain gH/gL/gp42-NP+gp350$D_{123}$-NP, respectively (Fig. 3B, right) and the activity was maintained for at least 12 weeks (data not shown). These findings were confirmed by measuring ELISA binding titers to gH/gL and gH/gL/gp42. In contrast, little reactivity to gp350$D_{123}$ was observed in pre-immune sera because the homology between EBV and rhLCV gp350 is much lower (49%) (Supplemental Fig 6, top and bottom right). gp350 is important for EBV attachment to B cells before the gH/gL/gp42 complex initiates membrane

fusion and is likely the reason why there was minimal difference in neutralization between B and epithelial cells. Regardless of prior immunity, anti-gH/gL, anti-gH/gL/gp42 and anti-gp350 antibody titers all increased after immunization (Supplemental Fig 6, **$p<0.0001$ or *$p<0.01$ respectively compared to pre-immune sera). These data confirmed the immunogenicity of bivalent single chain gH/gL-NP+gp350$D_{123}$-NP and single chain gH/gL/gp42-NP+gp350$D_{123}$-NP vaccines and indicate that neutralizing antibodies were induced by these vaccines in nonhuman primates. Although there is variation in antibody titers elicited by the bivalent vaccine in different models, our data clearly demonstrate that neutralizing antibodies could be readily elicited by the bivalent vaccines described in both naïve and EBV-immune animal models.

**Bivalent single chain gH/gL-NP+gp350$D_{123}$-NP or single chain gH/gL/gp42-NP+gp350$D_{123}$-NP immune sera protected humanized mice from EBV infection and lymphoma**

To assess the protective efficacy of single chain gH/gL-NP+gp350$D_{123}$-NP and single chain gH/gL/gp42-NP+gp350$D_{123}$-NP vaccines, we performed an EBV challenge study using a humanized mouse model. Engraftment of human CD34+ hematopoietic stem cells into NOD-scid IL2$rg^{-/-}$ mice (CD34+ huNSG) allows for the reconstitution of human immune system components and these mice can be infected with EBV (*18-21*). Purified IgG from naïve (control), single chain gH/gL-NP+gp350$D_{123}$-NP or single chain gH/gL/gp42-NP+gp350$D_{123}$-NP immunized BALB/c mice were passively transferred to three groups of CD34+ huNSG mice on days -1, 0 and +1 and mice were challenged intravenously with EBV on day 0. All animals in the control group had viremia while only one animal each receiving IgG from single chain gH/gL-NP+gp350$D_{123}$-NP or single chain gH/gL/gp42-NP+gp350$D_{123}$-NP immune animals had low level transient viremia on one day, further demonstrating the protective efficacy conferred by single chain gH/gL-NP+gp350$D_{123}$-NP and single chain gH/gL/gp42-NP+gp350$D_{123}$-NP vaccines (Fig. 4A, $p<0.05$ at

week 5 and week 9). In situ hybridization for EBV encoded RNA 1 (EBER1) showed viral RNA in tissue of 4 of 6 animals receiving control IgG, while tissues from all animals in the other two groups were entirely negative for EBER1 (Fig. 4B, $p<0.005$). Three of the six animals that received control IgG had EBV positive B cell lymphomas, while none of the animals that received IgG from either single chain gH/gL-NP+gp350$D_{123}$-NP or single chain gH/gL/gp42-NP+gp350$D_{123}$-NP immune animals developed lymphoma (Fig. 5 and Supplemental Fig. 7, $p<0.05$). We also determined the levels of anti-gH/gL, anti-gH/gL/gp42 and anti-gp350 in animals 1 week after challenge using an immunoprecipitation assay, and the antibody levels against gp350, gH/gL and gp42 were comparable to those from animals immunized with 2 doses of EBV vaccines in previous studies, ranging from $10^5$ to $10^6$ relative light units (Supplemental Fig. 8) (*14, 15*).

## DISCUSSION

An effective vaccine could reduce the burden of a variety of diseases associated with EBV infection, including infectious mononucleosis and a wide range of B cell and epithelial cell cancers. A previous phase 2 trial with an EBV gp350 vaccine reduced rate of infectious mononucleosis, but failed to induce sterilizing immunity in clinic (*10*), suggesting that additional immunogens that target viral entry to epithelial cells may be required for a successful prophylactic vaccine (*15, 22*). While EBV gp350 is important for attachment of the virus to B cells, it is not required for infection *in vitro*; in contrast, EBV gH, gL and gp42 are all essential for infection and EBV fusion to host cells. Here, we rationally designed vaccine candidates based on knowledge of their structural biology that allow expression of gH/gL and gH/gL/gp42 in a nanoparticle as a single polypeptide. This approach ensures the proper formation of 1:1 heterodimers for gH/gL and 1:1:1 heterotrimers for gH/gL/gp42, respectively. These single

chain recombinant proteins can be easily purified and the conformation of the gH/gL and gH/gL/gp42 nanoparticles remains intact compared with nanoparticles produced from combinations of polypeptides as determined by x-ray crystallography. The ability to express the gH/gL or gH/gL/gp42 nanoparticles as single polyproteins reduces the number of components required to generate the vaccines and enables greater control of product homogeneity that facilitates scaled manufacturing.

Immunization of mice with single chain gH/gL-NP or single chain gH/gL/gp42-NP induced high titers of antibodies that neutralized EBV entry to B cells and epithelial cells. Addition of a structurally optimized, truncated gp350, gp350$D_{123}$-NP (*14*), to single chain gH/gL-NP or single chain gH/gL/gp42-NP stimulated effective gp350 directed Abs without reducing gH/gL or gH/gL/gp42 responses as shown previously for gp350$D_{123}$-NP and gH/gL-NP or gH/gL/gp42-NP (*15*), suggesting that a bivalent vaccine formulation with both gp350 and gH/gL/gp42 components would provide improved coverage against the virus on different cell types. These neutralizing antibody responses were observed in ferrets, an EBV-naïve mammalian species. Importantly, in monkeys with pre-existing cross-reactive immunity to EBV due to prior infection by rhLCV, substantially higher titers of neutralizing antibodies were induced by immunization with these bivalent vaccines. In mice and NHPs, both single chain gH/gL-NP + gp350$D_{123}$-NP and gH/gL/gp42-NP + gp350$D_{123}$-NP bivalent vaccines induced neutralizing antibodies that inhibited EBV entry in B cells and epithelial cells. The neutralizing antibody levels ($IC_{50}$ titers) elicited by the bivalent vaccines were similar to those seen previously with combined gH/gL/gp42 + gp350 nanoparticle vaccines in other formats (*15*). Importantly, we show here that this immunity also protects against EBV infection and development of EBV lymphoma in vivo.

Evaluation of the protective efficacy of EBV vaccines is challenging as humans are the only natural reservoir for EBV. There are limitations in the animal models to evaluate EBV vaccine efficacy because EBV does not naturally infect rodents (*1*). In contrast, rhesus macaques are naturally infected almost universally by rhesus lymphocryptovirus (rhLCV) which is homologous to EBV; each of the rhLCV glycoproteins has an ortholog in EBV and antibodies to the rhLCV glycoproteins complicate EBV challenge studies. Furthermore, it is extremely difficult to obtain sufficient rhLCV seronegative NHPs for vaccination and challenge studies. Although vaccinated common marmosets have reduced EBV DNA in buccal fluid after EBV challenge (*23*), reduced shedding in oral fluids is not a useful test for efficacy of a vaccine. In addition, these animals are naturally infected with a marmoset homolog of EBV (*Callitrichine herpesvirus* 3) which has orthologs of EBV gH/gL/gp42 and gp350; thus, most common marmosets have antibodies to these glycoproteins that confound challenge studies. Finally, while rabbits can be infected with EBV, it requires non-physiologic, extremely high doses (20-80 million copies of EBV) of virus to infect them (*24*).

Several laboratories have modeled EBV infection in humanized mice engrafted with CD34+ hematopoietic progenitor cells isolated from umbilical cord blood (CD34+ huNSG) (*28*) and have shown that these animals become viremic after infection (*20*). Here we used this model to validate protection against EBV viremia using our bivalent EBV vaccines by passive transfer of immune IgG from vaccinated mice. Nearly all CD34+ huNSG mice that received purified IgG from bivalent vaccinated animals displayed undetectable viremia after EBV challenge; in contrast, $10^2$-$10^3$ copies of EBV DNA/10 µl of blood were present in animals that received control IgG. Successful protection was conferred by passive transfer of vaccine-induced antibodies. Because it is technically not possible to perform active immunization in a relevant

model of infection, we showed here that transfer of IgG obtained from serum alone conferred protection, demonstrating both the efficacy and mechanism of immune protection at the same time. There is ample precedent for the use of passive transfer to demonstrate vaccine-induced immune protection for other viruses (*25-27*). Similar to our previous report (*15*), both single chain gH/gL-NP and gH/gL/gp42-NP induced robust antibody responses that neutralized EBV entry to B cells and epithelial cells. The rationale to include gp42 is to mimic the natural heterotrimeric viral structure of the gH/gL/gp42 complex. This complex has been implicated in mediating B cell neutralization (*4*) and will be the lead candidate moving forward. Our approach ensures correct complex stoichiometry, simplifies protein production, minimizes heterogeneity, improves immunogen stability, and reduces manufacturing costs. Taken together, these data suggest that the single chain gH/gL/gp42 and gp350 bivalent vaccine represents an efficient, scalable candidate vaccine that is likely to limit viremia after EBV infection, thereby reducing infectious mononucleosis and possibly EBV associated cancers.

## MATERIALS AND METHODS

### Vector Construction.

The EBV glycoproteins gH, gL and gp42 amino acid sequences were obtained from NCBI GenPept with the following accession numbers: gH (Q3KSQ3.1), gL(P03212.1) and gp42 (P0C6Z5.1). Through structural modeling, the glycoproteins were fused via a flexible amino acid linker to make a single chain gH/gL heterodimer or gH/gL/gp42 heterotrimer recombinant protein (Supplementary Table 2). A 6-histidine tag with a thrombin cleavage sequence was placed at the C-terminus of the single chain recombinant protein for affinity purification purposes. The EBV nanoparticle glycoproteins were generated by fusing the singe-chain glycoproteins to the N-terminus of *Helicobacter pylori*- ferritin (*14*).

255

256 **Recombinant protein expression and purification**

257 Expi293F were transiently transfected using ExpiFectamine 293 reagent at a cell density
258 of 2 x $10^6$ cells/ml with the gH/gL, gH/gL/gp42, gH/gL nanoparticle, gH/gL/gp42 nanoparticle, or
259 gp350$D_{123}$ nanoparticle expression vector (Life Technologies). After 5 days of expression the
260 supernatants were harvested for purification. The gH/gL or gH/gL/gp42 constructs were affinity
261 tagged with a hexahistidine tag and was purified via Ni Sepharose 6 Fast Flow histidine-tagged
262 protein purification resin (GE Healthsciences). Nickel column eluate was concentrated to
263 approximately 10 mg/mL using 10 kDa cutoff centrifugal filters. This material was then subjected
264 to gel filtration chromatography using a HiLoad 16/600 Superdex 200pg column that had been
265 equilibrated in TBS buffer (20 mM Tris pH 7.4, 150 mM NaCl). Peak fractions containing pure
266 fusion protein (as judged by SDS-PAGE) were pooled and concentrated back to approximately 10
267 mg/mL. This sample was then deglycosylated by adding PNGase F enzyme at a ratio of 5 units
268 PNGase F per µg of fusion protein and incubated at room temperature for 72 hours. PNGase F was
269 then removed by gel filtration over a Superose 6 10/300 GL column equilibrated in TBS, pooling
270 non-void fractions containing the fusion protein, but not PNGase F. These fractions were
271 concentrated to 7.5 mg/mL and stored at 4°C. The nanoparticles were purified via ion exchange
272 chromatography (20 mM Tris-HCl pH 7.5, 50 mM NaCl), followed by Superose 6 10/300gL size
273 exclusion chromatography filtration column in PBS (GE Healthsciences). SDS-PAGE and western
274 blots were performed to detect the presence of the nanoparticles (Biorad). Endotoxin analyses
275 ensured that all vaccine doses contained <0.1 EU per mouse.

276 **Crystallization and cryoprotection**

277 Crystallization was carried out by sitting drop vapor diffusion at 18°C against a solution
278 of 0.1 M Bis-Tris pH 5.5, 0.375 M ammonium sulfate, and 19.5% PEG 3350 for single-chain

gH/gL/gp42 and 1M LiCl, 10% PEG 6k, 0.1M $Na_3$Citrate pH 5.0 for single-chain gH/gL. Drops (200 nL total volume) were set up at a 1:1 ratio of protein stock (7.5 mg/mL) and crystallization solutions. Crystals were cryo-protected by transfer into a fresh drop of the crystallization solution supplemented to 25% glycerol and incubated for 10 s immediately prior to freezing in liquid $N_2$. X-ray diffraction data for single chain gH/gL were collected at the Advanced Photon Source beamline LS-CAT 21-ID-D and on an EigerX 9M Detector (wavelength 1.1 Å). X-ray diffraction data for single chain gH/gL/gp42 were collected at Diamond Light Source beamline i24 on a Pilatus 3 6M detector (wavelength 0.9686 Å). Both datasets were indexed, integrated and scaled using XDS (*29, 30*). Initial phases were obtained by molecular replacement with Phaser (*31, 32*) using the 3PHF structure for single chain gH/gL and the gH/gL/gp42 domains of 5W0K for single chain gH/gL/gp42. Structures were modeled and refined using the programs COOT (*33*) and PHENIX (*34*).

**Negative stain transmission electron microscopy**

1 mg/mL of nanoparticle samples were sent to the Harvard Medical School Electron Microscopy Facility for negative stain transmission electron microscopy. The samples were stained with 0.75% uranyl formate and a TecnaiG$^2$ Spirit BioTWIN microscope was used to image the grids. The images were recorded with an AMT 2k charge-coupled device camera.

**Immunization**

Animal experiments were carried out in accordance with all federal regulations and were approved by the Sanofi Institutional Animal Care and Use Committee in fully AAALAC accredited facilities. Six- to eight-week old female BALB/c mice (Sanofi in house) were immunized (n=5) intramuscularly with purified proteins either in the absence or presence of Sanofi Pasteur AF03 adjuvant at 50% (v/v) formulation. 1 µg gH/gL or 1 µg gH/gL/gp42 nanoparticles plus 1 µg of

naked ferritin nanoparticle vaccine were given intramuscularly to each mouse. The bivalent formulation comprised 1 µg gH/gL or 1 µg gH/gL/gp42 nanoparticle plus 1 µg gp350D$_{123}$ nanoparticle vaccine. Immunizations were given at weeks 0 and 3. Sera were collected -2 days before immunization, and then at week 2, 5, and 8 post- immunizations. The animal studies with gH/gL and gH/gL/gp42 were performed in separate, independent experiments. Given the limited amount of sera available from these mice, it was technically not possible to perform neutralization assays for a head-to-head comparison.

Ferrets and NHP studies were carried out in accordance with the recommendations of the Association for Assessment and Accreditation of Laboratory Animal Care International Standards and with the recommendations in the Guide for the Care and Use of Laboratory Animals of the United States—National Institutes of Health. The Institutional Animal Use and Care Committee of BIOQUAL approved these experiments. Ferrets (n=6/group) were injected intramuscularly with 15 µg gH/gL or 15 µg gH/gL/gp42 nanoparticles plus 15 µg gp350D$_{123}$ nanoparticle vaccine in the presence of Sanofi Pasteur AF03 adjuvant at 50% (v/v) formulation at weeks 0 and 4. Sera were analyzed at weeks 0, 2, and 6. All rhesus macaques are considered rhLCV-seropositive as pre-immune sera showed high background against gH/gL and gH/gL/gp42 and residual activity against gp350 (Supplemental Figure 6). Rhesus macaques (n=4/group) were injected intramuscularly with 25 µg gH/gL or 25 µg gH/gL/gp42 nanoparticles plus 25 µg dose of gp350D$_{123}$ nanoparticle vaccine in the presence of Sanofi Pasteur AF03 adjuvant at 50% (v/v) formulation at weeks 0, 4, and 10. Sera were analyzed at weeks -1, 2, 6, 8, and 12.

**Enzyme-linked immunosorbent assay**

Plates were coated with antigens at 100 ng/well in PBS and incubated at 4°C overnight. The plates were then washed five times in PBS-T and blocked with buffer containing 5% milk (Difco #232100) and 1% BSA (Sigma #A906-500G) in PBS-T (BioVision #2310-100). Serial

dilutions of serum were made in 2.5% milk and 0.5% BSA in PBS-T. The diluted sera were added to the plate and incubated for 1 hour at room temp before being washed five times in PBS-T. Anti-mouse-HRP secondary (GE NA931V), anti-NHP-HRP secondary (Invitrogen), or HRP anti-ferret IgG (LS Bio LS-C61236-1) were added to the plate, and incubated for 1 hour at room temperature. The plate was washed five times and Sure Blue Substrate (KPL #52-00-00) was added at 100 µL/well. Once color was visualized, the reaction was stopped by adding 100 µL of 1N $H_2SO_4$ and a Spectramax M5 plate reader was used to measure absorbency at 450nm.

**GFP reporter virus neutralization assay**

Immune sera from vaccinated mice, ferrets, or monkeys were serial diluted and incubated with B95-8/F EBV GFP-reporter virus for 2 hours. The mixture was added to Raji B cells, SVK CR2 or 293 epithelial cells and incubated for 3 days (*15*). Cells were then washed and fixed for flow cytometry to measure for GFP-positive cells

**Quantification of antibody titers in plasma by luciferase immunoprecipitation system assay**

EBV gp350, gH/gL, and gp42 antibody titers in the week 1 post EBV challenge plasma samples were measured by luciferase immunoprecipitation system (LIPS) assay as previously described (*35, 36*). Briefly, cell lysates expressing EBV gp350, gH/gL, or gp42 Renilla luciferase fusion proteins were incubated with plasma from week 1 post infection for 1 hr and immunoprecipitated with protein A/G beads for 1 hr. Coelenterazine substrate was added to each well and luciferase activity was measured in light units (LU) by a luminometer. Each sample was tested in duplicate. The inoculum for the passive transfer in vivo study, purified IgG from single chain gH/gL-NP+gp350$D_{123}$-NP or single chain gH/gL/gp42-NP+gp350$D_{123}$-NP immunized BALB/c mice, was serially diluted and used to generate a standard curve. Plasma from mice 1 week post EBV challenge that received purified IgG from naïve BALB/C mice were included in

each plate as a negative control. LU values that were in the linear range of a standard curve were converted to antibody titers in the plasma by interpolating a standard curve using GraphPad PRISM software.

**Passive transfer EBV challenge study**

Humanized mouse experiments were carried out in accordance with federal regulations and NIH guidelines and were approved by the Animal Care and Use Committee of the National Institute of Allergy and Infectious Diseases. Three groups of BALB/c mice (n=80/group) were immunized with 5 µg gH/gL or 5 µg gH/gL/gp42 nanoparticle plus 5 µg dose of $gp350D_{123}$ in the presence of AF03 adjuvant at weeks 0, 3 and 7 to induce an antibody response. Sera from each of the vaccinated BALB/C groups were pooled at weeks 4, 5, 8, 9, and 10 for mouse IgG purification. The control group was unimmunized BALB/c mice; similar non-immune sera have often been used as a negative control in previous publications (*37, 38*). Purified mIgG from each group was passively transferred to CD34+ humanized NSG mice (Jackson Laboratory) intraperitoneally at 20 µg of mIgG per gram of mouse at day -1, day 0, and day 1. The mice were challenged intravenously at day 0 with $10^5$ Green Raji Units of EBV. Mice were weighed weekly. EBV viremia was measured using qPCR to detect the viral gene BamH1 W (*39*) in the blood at week 5, 7, 9, 14, and 18.

**Dynamic light scattering**

DLS measurements were performed at 25°C using a DynaPro Plate Reader II (Wyatt Technology). The samples were diluted in PBS, adjusted to 0.01 mg/mL concentration for each measurement. The average particle size was quantified from ten measurements.

**Immunohistochemistry**

Tissues from mice were collected 27 weeks after EBV challenge and fixed in 10% neutral-buffered formalin. Sections were stained with hematoxylin and eosin, antibody to human CD20 followed by 3,3' diaminobenzidine as a chromogen, and in situ hybridization was performed using a riboprobe for EBV EBER1. Sections were coded and read by a pathologist in a blinded fashion.

**Statistics**

*P*-values were derived by Student's *t* test or Fisher's exact test with GraphPad PRISM version 9.3.

**Funding:** this study was funded by Sanofi R&D and the Intramural Research Program of the National Institute of Allergy and Infectious Diseases.

**Acknowledgements** We thank all members of Sanofi Breakthrough Lab for insightful discussions throughout this study. We thank Hanne Andersen Elyard, Laurent Pessaint and Jake Yalley from Bioqual for assistance with Ferret and NHP studies. We thank Harvard Medical School Electron Microscopy Facility for negative stain transmission electron microscopy. We thank Amy Sullivan, Kelly Balko, and the Sanofi Comparative Medicine group for help with the mouse immunogenicity studies,

**Author contributions:** C.-J. W., W.B., L.A.N., J.I.C., and G.J.N. designed research studies; L.A.N., W.B., J.D.B, R.K., S.P.; J.R.F., T.-H.C. performed the research; L.A.N., C.-J. W., W.B., J.D.B., R.K., S.P.; J.R.F., J.I.C., and G.J.N. interpreted and discussed the data; C.-J. W., W.B., L.A.N., J.I.C., and G.J.N. wrote the paper and all authors participated in manuscript revisions.

**Competing interests:** At the time the research described in this paper was initiated, L.A.N., C.-J. W., J.D.B., J.R.F., T.-H. C. and G.J.N. were employees of Sanofi which has filed patent applications on EBV vaccines. C.J.W. and G.J.N. are inventors of nanoparticle-based vaccines that have been filed by either Sanofi or the U.S. government. W.B and J.I.C. are current

394 employees of U.S. government which has issued patents on ferritin-nanoparticle based EBV
395 vaccines.

396 **Data and materials availability:** All data is available in the main text or the supplementary
397 materials.

398 **Supplementary Materials (on a separate file):**

399 Materials and Methods

400 Figs. S1 to S9

401 Tables S1 to S2

402

## FIGURES LEGENDS

**Figure 1. Structure-based design of single chain gH/gL and single chain gH/gL/gp42 nanoparticles.** **(A)** A schematic representation of the single chain gH/gL, single chain gH/gL/gp42, single chain gH/gL-NP, and single chain gH/gL/gp42-NP. EBV gL (green) is fused to the N terminus of gH (cyan) via a flexible amino acid linker (indicated by the black line between gL and gH). EBV gp42 (gray) is fused to the C-terminus of gH. Single chain gH/gL-NP or single chain gH/gL/gp42-NP constructs show the gH/gL or gH/gL/gp42 fused to *H. pylori* ferritin (represented by the letter "F" in beige) by a flexible amino acid linker (line), respectively. **(B)** Left: The crystal structure of the single chain gH/gL was resolved at 5.5Å (gL in green and gH in cyan) with superposition of the previously solved crystal structure of gH/gL complex (white, PDB: 3PHF) (RMS = 0.33). Right: The crystal structure of the single chain gH/gL/gp42 was resolved at 2.9Å and superposition with the previously solved heterotrimer gH/gL/gp42 complex crystal structure (white, PDB: 5T1D) (RMS value = 0.96). **(C)** Left: Size exclusion chromatography (SEC) elution profiles of single chain gH/gL-NP and single chain gH/gL/gp42-NP. Right: Size of single chain gH/gL-NP and single chain gH/gL/gp42-NP determined by DLS. **(D)** Negative stain EM image of single chain gH/gL-NP and single chain gH/gL/gp42-NP. A close-up image of the nanoparticle is displayed at the upper right corner. A structural model of the single chain gH/gL-NP or single chain gH/gL/gp42-NP is shown on the right of the EM image (gH: cyan; gL: green; gp42: gray; ferritin: orange). The surface density is a model built from crystal structures solved in panel B and ferritin core from PDB 3BVE (DOI:10.2210/pdb3bve/pdb) using Chimera (*40*) and is not reconstructed from EM.

**Figure 2. Neutralization responses induced by single chain gH/gL-NP or single chain gH/gL/gp42-NP alone or in combination with gp350D$_{123}$-NP in mice.**

BALB/C mice (n=5/group) were immunized intramuscularly in the presence of AF03 adjuvant at weeks 0 and 3 with 1µg of **(A)** monovalent single chain gH/gL-NP, gp350D$_{123}$ or bivalent gH/gL-NP+gp350D$_{123}$-NP or **(B)** monovalent single chain gH/gL/gp42-NP or bivalent gH/gL/gp42-NP+gp350D$_{123}$-NP. Control is pre-immune sera. Neutralization antibody titers from immune sera collected 2 weeks after the 2$^{nd}$ injection was determined in Raji B cells and SVK CR2 epithelial cells. The IC$_{50}$ indicated the log titer that resulted in 50% inhibition of EBV entry into target cells. The data are shown as box-and-whiskers plots (box indicates lower and upper quartiles with line at median, and whiskers span minimum and maximum data points; *p<0.05 compared to control).

**Figure 3. Immunogenicity of single chain gH/gL-NP+gp350D$_{123}$-NP or single chain gH/gL/gp42-NP alone or in combination with gp350D$_{123}$-NP in ferrets and NHP.**

**(A)** Ferrets were immunized intramuscularly at weeks 0 and 4 with either 15 µg single chain gH/gL-NP + 15 µg gp350D$_{123}$-NP or 15 µg single chain gH/gL/gp42-NP + 15 µg gp350D$_{123}$-NP bivalent vaccines. Sera were collected 2 weeks after immunization and were assayed for neutralizing activity in both Raji B cells (left) and 293 epithelial cells (right). Means and standard deviations are shown (* p< 0.05 compared to pre-immune sera). No neutralizing activity was detected from the pre-immune sera and levels were at the limit of detection in the graphs. **(B)** Rhesus macaques (n=4/group) were vaccinated with the bivalent vaccine composed of 25µg gH/gL-NP + 25µg gp350D$_{123}$-NP or 25µg gH/gL/gp42-NP + 25µg gp350D$_{123}$-NP at weeks 0, 4, and 10. AF03 was used as adjuvant. Immune sera were collected 2 weeks after the 3$^{rd}$ injection

449 and neutralizing antibody titers were determined in both Raji B cells and SVK CR2 epithelial cells.
450 Means and standard deviations are shown (* $p < 0.05$ compared to pre-immune sera).
451
452 **Figure 4. Immune protection by passive transfer of bivalent vaccine sera against EBV**
453 **infection in humanized NSG mice.**
454 Humanized NSG mice (n=6/group) were injected IgG (20μg/g of mouse body weight)
455 purified from naïve (control), single chain gH/gL-NP+ gp350$D_{123}$-NP or single chain
456 gH/gL/gp42+gp350$D_{123}$-NP immunized BALB/C mice. Passive transfer of IgG was delivered
457 intraperitoneally on day -1, 0 and 1 and EBV challenge was performed intravenously on day 0.
458 **(A)** Viremia from each group was measured at weeks 5 7, and 9 post challenge. Medians with 25%
459 and 75% percentiles are shown (* $p < 0.05$ compared to control at the same week). **(B)** Heatmap
460 showing EBV encoded RNA 1 (EBER1) positivity of tissues (graded 0 to 3) from mice receiving
461 IgG from naïve, single chain gH/gL-NP+ gp350$D_{123}$-NP, or single chain gH/gL/gp42+gp350$D_{123}$-
462 NP immunized BALB/C mice after challenge with EBV. A score of 0 indicates no EBER1 staining
463 while a score of 3 indicates marked infiltration of tissues by EBER1-positive cells.
464
465 **Figure 5. Protection against EBV lymphoma *in vivo*.**
466 Pathologic and immunohistochemical analysis of the liver from representative mice
467 receiving IgG from non-immune (Control, left) or vaccinated mice (Immune, middle and right)
468 after challenge with EBV. Tissues were collected 27 weeks after challenge and stained with
469 hematoxylin and eosin (H&E, yellow arrows indicate representative region with lymphoma) or
470 anti-CD20 antibody (brown staining, red arrows), or in situ hybridization was performed with a
471 probe to EBER1 (purple staining, red arrows). CD20 and EBER staining are apparent in control,

472 but not in any of the tissues receiving IgG from vaccinated mice. No EBV-positive B cell
473 lymphomas were observed in the latter animals.
474

475 **Table S1. Data collection and refinement statistics (molecular replacement)**

| | Single chain gH/gL/gp42 | Single chain gH/gL/ |
|---|---|---|
| **Data collection** | | |
| Space group | P 21 21 21 | C2 |
| Cell dimensions | | |
| *a*, *b*, *c* (Å) | 89.85, 120.94, 143.65 | 543.4, 167.4, 383.6 |
| α, β, γ (°) | 90 90 90 | 90 134 90 |
| Resolution (Å) | 89.85 - 2.87 (2.94 - 2.87) | 195 – 5.5 (5.52 – 5.5) |
| $R_{merge}$ | 0.148 (2.024) | 0.095 (1.26) |
| $R_{meas}$ | 0.161 (2.202) | 0.116 (1.42) |
| $I / \sigma I$ | 9.2 (1.0) | 8.2 (1.0) |
| $CC_{1/2}$ | 0.997 (0.401) | 0.992 (0.329) |
| Completeness (%) | 99.9 (100.0) | 97.9 (92.7) |
| Redundancy | 6.4 (6.5) | 3.9 (3.4) |
| **Refinement** | | |
| Resolution (Å) | 61.76 – 2.87 (2.973 – 2.87) | 136.2 – 5.5 (5.64 – 5.5) |
| No. reflections | 36423 (3580) | 76750 (5476) |
| $R_{work}$ / $R_{free}$ | 0.2241 / 0.2520 (0.3500 / 0.4206) | 0.299 / 0.338 (0.38 / 0.395) |
| No. atoms | 7437 | 85882 |
| Protein | 7293 | 85882 |
| Ligand/ion | 144 | 0 |
| Water | 0 | 0 |
| *B*-factor | 85.83 | 279.3 |
| Protein | 84.86 | 279.3 |
| Ligand/ion | 119.27 | N/A |
| Ramachandran | | |
| Favored (%) | 96.62 | 92.9 |
| Allowed (%) | 3.38 | 6.72 |
| Outlier (%) | 0.00 | 0.28 |
| R.m.s. deviations | | |
| Bond lengths (Å) | 0.002 | 0.002 |
| Bond angles (°) | 0.48 | 1.220 |
| Molprobity | | |
| Clashscore | 2.78 | 10.79 |
| Rotamer outliers (%) | 0.99 | 2.2 |
| Cβ deviations | 0 | 0.03 |
| Cis-proline (%) | 0.00 | 0.00 |
| Twisted proline (%) | 0.00 | 0.21 |

476 *Values in parentheses refer to the highest-resolution shell.

477

478

479

480

481

482

483

484

485

486

## Table S2. Amino acid sequences of constructs used

| Construct | Key:<br>Leader Sequence – underlined<br>gL – *Italicized*<br>Linker – double underlined<br>gH – Bold<br>bfpFerr (ferritin) – wavy underline<br>gp350D$_{123}$ – *Italicized and bold*<br>gp42 – *Italicized and underlined*<br>Thrombin cleavage site: *Italicized and dashed underline*<br>6X His Tag: *Bold, italicized and curvy underline* |
|---|---|
| gp350D$_{123}$ monomer | MDSKGSSQKGSRLLLLLVVSNLLLPQGVLA***EAALLVCQYTIQSLIHLTGEDPGFFNV EIPEFPFYPTCNVCTADVNVTINFDVGGKKHQLDLDFGQLTPHTKAVYQPRGAFGGS ENATNLFLLELLGAGELALTMRSKKLPINVTTGEEQQVSLESVDVYFQDVFGTMWC HHAEMQNPVYLIPETVPYIKWDNCNSTNITAVVRAQGLDVTLPLSLPTSAQDSNFSV KTEMLGNEIDIECIMEDGEISQVLPGDNKFNITCSGYESHVPSGGILTSTSPVATPIPG TGYAYSLRLTPRPVSRFLGNNSILYVFYSGNGPKASGGDYCIQSNIVFSDEIPASQDMP TNTTDITYVGDNATYSVPMVTSEDANSPNVTVTAFWAWPNNTETDFKCKWTLTSGT PSGCENISGAFASNRTFDITVSGLGTAPKTLIITRTATNATTTTHKVIFSKAPE***GSGSGS GLVPRGSGAGGG***HHHHHH*** |
| gH/gL monomer | MRAVGVFLAICLVTIFVLPTWG*NWAYPCCHVTQLRAQHLLALENISDIYLVSNQTCDGFS LASLNSPKNGSNQLVISRCANGLNVVSFFISILKRSSSALTGHLRELLTTLETLYGSFSVEDLF GANLNRYAWHRGG*GGSGSGSNSSASSGASSGGASGGSGGSG**AASLSEVKLHLDIEG HASHYTIPWTELMAKVPGLSPEALWREANVTEDLASMLNRYKLIYKTSGTLGIA LAEPVDIPAVSEGSMQVDASKVHPGVISGLNSPACMLSAPLEKQLFYYIGTMLPN TRPHSYVFYQLRCHLSYVALSINGDKFQYTGAMTSKFLMGTYKRVTEKGDEHV LSLVFGKTKDLPDLRGPFSYPSLTSAQSGDYSLVIVTTFVHYANFHNYFVPNLKD MFSRAVTMTAASYARYVLQKLVLLEMKGGCREPELDTETLTTMFEVSVAFFKV GHAVGETGNGCVDLRWLAKSFFELTVLKDIIGICYGATVKGMQSYGLERLAAM LMATVKMEELGHLTTEKQEYALRLATVGYPKAGVYSGLIGGATSVLLSAYNRH PLFQPLHTVMRETLFIGSHVVLRELRLNVTTQGPNLALYQLLSTALCSALEIGEV LRGLALGTESGLFSPCYLSLRFDLTRDKLLSMAPQEATLDQAAVSNAVDGFLGR LSLEREDRDAWHLPAYKCVDRLDKVLMIIPLINVTFIISSDREVRGSALYEASTTY LSSSLFLSPVIMNKCSQGAVAGEPRQIPKIQNFTRTQKSCIFCGFALLSYDEKEGL ETTTYITSQEVQNSILSSNYFDFDNLHVHYLLLTTNGTVMEIAGLYEERA*SGSGS GSG*LVPRGS*GAGGG***HHHHHH*** |
| gL/gH/gp42 monomer | MRAVGVFLAICLVTIFVLPTWG*NWAYPCCHVTQLRAQHLLALENISDIYLVSNQTCDGFS LASLNSPKNGSNQLVISRCANGLNVVSFFISILKRSSSALTGHLRELLTTLETLYGSFSVEDLF GANLNRYAWHRGG*GGSGSASSGASASGSSNGSGSGSGSNSSASSGASSGGASGGSGG SG**AASLSEVKLHLDIEGHASHYTIPWTELMAKVPGLSPEALWREANVTEDLASM LNRYKLIYKTSGTLGIALAEPVDIPAVSEGSMQVDASKVHPGVISGLNSPACMLS APLEKQLFYYIGTMLPNTRPHSYVFYQLRAHLSYVALSINGDKFQYTGAMTSKF LMGTYKRVTEKGDEHVLSLVFGKTKDLPDLRGPFSYPSLTSAQSGDYSLVIVTT FVHYANFHNYFVPNLKDMFSRAVTMTAASYARYVLQKLVLLEMKGGCREPEL DTETLTTMFEVSVAFFKVGHAVGETGNGCVDLRWLAKSFFELTVLKDIIGICYG ATVKGMQSYGLERLAAMLMATVKMEELGHLTTEKQEYALRLATVGYPKAGV YSGLIGGATSVLLSAYNRHPLFQPLHTVMRETLFIGSHVVLRELRLNVTTQGPN LALYQLLSTALCSALEIGEVLRGLALGTESGLFSPCYLSLRFDLTRDKLLSMAPQ EATLDQAAVSNAVDGFLGRLSLEREDRDAWHLPAYKCVDRLDKVLMIIPLINVT FIISSDREVRGSALYEASTTYLSSSLFLSPVIMNKCSQGAVAGEPRQIPKIQNFTRT QKSCIFCGFALLSYDEKEGLETTTYITSQEVQNSILSSNYFDFDNLHVHYLLLTTN GTVMEIAGLYEERA*SGGGSGSASSGASASGSSGSGSGSGSSSASSG*LAYFLPPRVRGG GRVAAAAITWVPKPNVEVWPVDPPPPVNFNKTAEQEYGDKEVKLPHWTPTLHTFQVPQN YTKANCTYCNTREYTFSYKGCCFYFTKKKHTWNGCFQACAELYPCTYFYGPTPDILPVVTR |

| | |
|---|---|
| | *NLNAIESLWVGVYRVGEGNWTSLDGGTFKVYQIFGSHCTYVSKFSTVPVSHHECSFLKPCL CVSQRSNSGSHHHHHH* |
| gp350D$_{123}$ nanoparticle | MDSKGSSQKGSRLLLLLVVSNLLLPQGVLA***EAALLVCQYTIQSLIHLTGEDPGFFNV EIPEFPFYPTCNVCTADVNVTINFDVGGKKHQLDLDFGQLTPHTKAVYQPRGAFGGS ENATNLFLLELLGAGELALTMRSKKLPINVTTGEEQQVSLESVDVYFQDVFGTMWC HHAEMQNPVYLIPETVPYIKWDNCNSTNITAVVRAQGLDVTLPLSLPTSAQDSNFSV KTEMLGNEIDIECIMEDGEISQVLPGDNKFNITCSGYESHVPSGGILTSTSPVATPIPG TGYAYSLRLTPRPVSRFLGNNSILYVFYSGNGPKASGGDYCIQSNIVFSDEIPASQDMP TNTTDITYVGDNATYSVPMVTSEDANSPNVTVTAFWAWPNNTETDFKCKWTLTSGT PSGCENISGAFASNRTFDITVSGLGTAPKTLIITRTATNATTTHKVIFSKAPE***GSESQV RQQFSKDIEKLLNEQVNKEMQSSNLYMSMSSWSYTHSLDGAGLFLFDHAAEEYEHA KKLIIFLNENNVPVQLTSISAPEHKFEGLTQIFQKAYEHEQHISESINNIVDHAIKCKDH ATFNFLQWYVAEQHEEEVLFKDILDKIELIGNENHGLYLADQYVKGIAKSRKS |
| gH/gL nanoparticle | MRAVGVFLAICLVTIFVLPTWG*NWAYPCCHVTQLRAQHLLALENISDIYLVSNQTCDGFS LASLNSPKNGSNQLVISRCANGLNVVSFFISILKRSSSALTGHLRELLTTLETLYGSFSVEDLF GANLNRYAWHRGG*GGSGSASSGASASGSSNGSGSGSGSNSSASSGASSGGASGGSGG SG**AASLSEVKLHLDIEGHASHYTIPWTELMAKVPGLSPEALWREANVTEDLASM LNRYKLIYKTSGTLGIALAEPVDIPAVSEGSMQVDASKVHPGVISGLNSPACMLS APLEKQLFYYIGTMLPNTRPHSYVFYQLRAHLSYVALSINGDKFQYTGAMTSKF LMGTYKRVTEKGDEHVLSLVFGKTKDLPDLRGPFSYPSLTSAQSGDYSLVIVTT FVHYANFHNYFVPNLKDMFSRAVTMTAASYARYVLQKLVLLEMKGGCREPEL DTETLTTMFEVSVAFFKVGHAVGETGNGCVDLRWLAKSFFELTVLKDIIGICYG ATVKGMQSYGLERLAAMLMATVKMEELGHLTTEKQEYALRLATVGYPKAGV YSGLIGGATSVLLSAYNRHPLFQPLHTVMRETLFIGSHVVLRELRLNVTTQGPN LALYQLLSTALCSALEIGEVLRGLALGTESGLFSPCYLSLRFDLTRDKLLSMAPQ EATLDQAAVSNAVDGFLGRLSLEREDRDAWHLPAYKCVDRLDKVLMIIPLINVT FIISSDREVRGSALYEASTTYLSSSLFLSPVIMNKCSQGAVAGEPRQIPKIQNFTRT QKSCIFCGFALLSYDEKEGLETTTYITSQEVQNSILSSNYFDFDNLHVHYLLLTTN GTVMEIAGLYEERA**SGGGSGSASSGASASGSSGSGSGSGSSSASSGASSGGASGGGS GGSGESQVRQQFSKDIEKLLNEQVNKEMQSSNLYMSMSSWSYTHSLDGAGLFLFDH AAEEYEHAKKLIIFLNENNVPVQLTSISAPEHKFEGLTQIFQKAYEHEQHISESINNIVD HAIKCKDHATFNFLQWYVAEQHEEEVLFKDILDKIELIGNENHGLYLADQYVKGIAK SRKS |
| gH/gL/gp42 nanoparticle | MRAVGVFLAICLVTIFVLPTWG*NWAYPCCHVTQLRAQHLLALENISDIYLVSNQTCDGFS LASLNSPKNGSNQLVISRCANGLNVVSFFISILKRSSSALTGHLRELLTTLETLYGSFSVEDLF GANLNRYAWHRGG*GGSGSASSGASASGSSNGSGSGSGSNSSASSGASSGGASGGSGG SG**AASLSEVKLHLDIEGHASHYTIPWTELMAKVPGLSPEALWREANVTEDLASM LNRYKLIYKTSGTLGIALAEPVDIPAVSEGSMQVDASKVHPGVISGLNSPACMLS APLEKQLFYYIGTMLPNTRPHSYVFYQLRAHLSYVALSINGDKFQYTGAMTSKF LMGTYKRVTEKGDEHVLSLVFGKTKDLPDLRGPFSYPSLTSAQSGDYSLVIVTT FVHYANFHNYFVPNLKDMFSRAVTMTAASYARYVLQKLVLLEMKGGCREPEL DTETLTTMFEVSVAFFKVGHAVGETGNGCVDLRWLAKSFFELTVLKDIIGICYG ATVKGMQSYGLERLAAMLMATVKMEELGHLTTEKQEYALRLATVGYPKAGV YSGLIGGATSVLLSAYNRHPLFQPLHTVMRETLFIGSHVVLRELRLNVTTQGPN LALYQLLSTALCSALEIGEVLRGLALGTESGLFSPCYLSLRFDLTRDKLLSMAPQ EATLDQAAVSNAVDGFLGRLSLEREDRDAWHLPAYKCVDRLDKVLMIIPLINVT FIISSDREVRGSALYEASTTYLSSSLFLSPVIMNKCSQGAVAGEPRQIPKIQNFTRT QKSCIFCGFALLSYDEKEGLETTTYITSQEVQNSILSSNYFDFDNLHVHYLLLTTN GTVMEIAGLYEERA**SGGGSGSASSGASASGSSGSGSGSGSSSASSG*LAYFLPPRVRGG GRVAAAAITWVPKPNVEVWPVDPPPPVNFNKTAEQEYGDKEVKLPHWTPTLHTFQVPQN YTKANCTYCNTREYTFSYKGCCFYFTKKKHTWNGCFQACAELYPCTYFYGPTPDILPVVTR NLNAIESLWVGVYRVGEGNWTSLDGGTFKVYQIFGSHCTYVSKFSTVPVSHHECSFLKPCL CVSQRSNS*GGSGSASSGASASGSSGSGSGSGSSSASSGASSGGASGGSGGSGGGSGSA SSGASASGSSGSGSGSGSSSASSGASSGGASGGSGGSGESQVRQQFSKDIEKLLNEQV NKEMQSSNLYMSMSSWSYTHSLDGAGLFLFDHAAEEYEHAKKLIIFLNENNVPVQL |

| | |
|---|---|
| | TSISAPEHKFEGLTQIFQKAYEHEQHISESINNIVDHAIKCKDHATFNFLQWYVAEQHEEEVLFKDILDKIELIGNENHGLYLADQYVKGIAKSRKS |

488

489

# SUPPLEMENTAL FIGURES

**Supplemental Figure 1. Expression of single chain gH/gL and single chain gH/gL/gp42 constructs.**

(A.) SDS-PAGE analysis of purified single chain gH/gL and single chain gH/gL/gp42 constructs.

(B.) SDS-PAGE of purified single chain gH/gL-NP and single chain gH/gL/gp42-NP.

**Supplemental Figure 2. Immunogenicity of single chain gH/gL-NP with or without AF03 adjuvant.**

Mice were immunized at week 0 and week 3. Immune sera were collected at weeks 0, 2 and 5 and antibody titers were determined by ELISA. Mean and standard error are shown. The p value from week 5 was <0.0001.

**Supplemental Figure 3. Immunogenicity of single chain gH/gL-NP and gp350D$_{123}$-NP in mice.**

A monovalent single chain gH/gL-NP or gp350D$_{123}$-NP, or bivalent single chain gH/gL-NP+gp350D$_{123}$-NP was used to immunize mice with AF03 as adjuvant. Antibody titers pre- and post-immunization against either (a) gH/gL heterodimer or (b) gp350D$_{123}$ were determined by ELISA. The data are shown as box-and-whiskers plots (box indicates lower and upper quartiles with line at median, and whiskers span minimum and maximum data points; *p<0.0001 compared to pre-immune sera).

**Supplemental Figure 4. Immunogenicity of single chain gH/gL/gp42-NP with gp350D$_{123}$-NP in mice.**

Monovalent single chain gH/gLgp42-NP (a) or bivalent single chain gH/gL-NP/gp42-NP+gp350D$_{123}$-NP (b) was used to immunize mice with AF03 as adjuvant. Antibody titers from immune sera collected 2 weeks after first and second immunizations against either gH/gL heterodimer, gp42 or gp350D$_{123}$ were determined by ELISA. The data are shown as box-and-whiskers plots (box indicates lower and upper quartiles with line at median, and whiskers span minimum and maximum data points; *$p<0.0001$ compared to week 2 sera).

**Supplemental Figure 5. Immunogenicity of single chain gH/gL-NP+gp350D$_{123}$-NP and single chain gH/gL/gp42-NP+gp350D$_{123}$-NP vaccines in ferrets.**

Ferrets (n=6/group) were immunized with either (a) bivalent gH/gL-NP+gp350D$_{123}$-NP or (b) bivalent gH/gL/gp42-NP+gp350D$_{123}$-NP vaccines at weeks 0 and 4. Binding antibody titers to gH/gL, gp350D$_{123}$, and gp42 were determined. Means and standard deviations are shown (**$p<0.0001$ or *$p<0.05$ respectively compared to pre-immune sera).

**Supplemental Figure 6. Immunogenicity of single chain gH/gL-NP+gp350D$_{123}$-NP and single chain gH/gL/gp42-NP+gp350D$_{123}$-NP vaccines in nonhuman primates.**

Rhesus macaques were immunized with either (a) single chain gH/gL-NP+gp350D$_{123}$-NP or (b) single chain gH/gL/gp42-NP+gp350D$_{123}$-NP bivalent vaccines at weeks 0, 4, and 10. Pre- and post-immunization binding antibody titers against gH/gL or gH/gL/gp42 or gp350D$_{123}$ were determined by ELISA. Means and standard deviations are shown (**$p<0.0001$ or *$p<0.01$ respectively compared to pre-immune sera).

**Supplemental Figure 7. EBV lymphoma in challenged humanized mice.** EBV-positive B cell lymphomas and CD20 and EBER positive cells were observed in the (a) spleen and (b) kidney of mice receiving IgG from naïve BALB/C after EBV challenge (Control). No evidence of EBV-positive B cell lymphomas was seen in mice receiving IgG from animals vaccinated with single chain gH/gL-NP+gp350$D_{123}$-NP or gH/gL/gp42-NP+gp350$D_{123}$-NP (Immune). CD20 staining and EBER are also negative in these mice. Tissues were harvested and stained as in Fig. 5. Arrows indicate representative areas of pathology and staining for the indicated cellular or viral proteins.

**Supplemental Figure 8. Anti-gH, gL, and gp42 antibody levels in mice challenged with EBV.** Antibody titers in plasma samples of humanized mice receiving IgG from vaccinated or naïve (control) mice obtained one week after challenge were measured by LIPS assay and shown as RLUs. Antibody titers in animals that received IgG from naïve, single chain gH/gL-NP+gp350D123-NP, and gH/gL/gp42-NP+gp350D123-NP immunized BALB/c mice are shown. Each symbol indicates one mouse. Minimum and maximum data points are represented by whiskers and box represents upper and lower quartiles with the horizontal line at the median.

555 **REFERENCES**


556 1. J. I. Cohen, E. S. Mocarski, N. Raab-Traub, L. Corey, G. J. Nabel, The need and
557 challenges for development of an Epstein-Barr virus vaccine. *Vaccine* **31 Suppl 2**, B194-
558 196 (2013).
559 2. J. I. Cohen, A. S. Fauci, H. Varmus, G. J. Nabel, Epstein-Barr virus: an important vaccine
560 target for cancer prevention. *Sci Transl Med* **3**, 107fs107 (2011).
561 3. D. Dierickx, T. M. Habermann, Post-Transplantation Lymphoproliferative Disorders in
562 Adults. *N Engl J Med* **378**, 549-562 (2018).
563 4. J. I. Cohen, Epstein-barr virus vaccines. *Clin Transl Immunology* **4**, e32 (2015).
564 5. J. D. Fingeroth *et al.*, Epstein-Barr virus receptor of human B lymphocytes is the C3d
565 receptor CR2. *Proc Natl Acad Sci U S A* **81**, 4510-4514 (1984).
566 6. M. K. Spriggs *et al.*, The extracellular domain of the Epstein-Barr virus BZLF2 protein
567 binds the HLA-DR beta chain and inhibits antigen presentation. *J Virol* **70**, 5557-5563
568 (1996).
569 7. J. I. Cohen, Vaccine Development for Epstein-Barr Virus. *Adv Exp Med Biol* **1045**, 477-
570 493 (2018).
571 8. J. Chen *et al.*, Ephrin receptor A2 is a functional entry receptor for Epstein-Barr virus.
572 *Nat Microbiol* **3**, 172-180 (2018).
573 9. H. Zhang *et al.*, Ephrin receptor A2 is an epithelial cell receptor for Epstein-Barr virus
574 entry. *Nat Microbiol* **3**, 1-8 (2018).
575 10. E. M. Sokal *et al.*, Recombinant gp350 vaccine for infectious mononucleosis: a phase 2,
576 randomized, double-blind, placebo-controlled trial to evaluate the safety,
577 immunogenicity, and efficacy of an Epstein-Barr virus vaccine in healthy young adults. *J*
578 *Infect Dis* **196**, 1749-1753 (2007).
579 11. M. A. Epstein, A. J. Morgan, S. Finerty, B. J. Randle, J. K. Kirkwood, Protection of
580 cottontop tamarins against Epstein-Barr virus-induced malignant lymphoma by a
581 prototype subunit vaccine. *Nature* **318**, 287-289 (1985).
582 12. J. Sashihara *et al.*, Soluble rhesus lymphocryptovirus gp350 protects against infection and
583 reduces viral loads in animals that become infected with virus after challenge. *PLoS*
584 *Pathog* **7**, e1002308 (2011).
585 13. X. Cui *et al.*, Rabbits immunized with Epstein-Barr virus gH/gL or gB recombinant
586 proteins elicit higher serum virus neutralizing activity than gp350. *Vaccine* **34**, 4050-
587 4055 (2016).
588 14. M. Kanekiyo *et al.*, Rational Design of an Epstein-Barr Virus Vaccine Targeting the
589 Receptor-Binding Site. *Cell* **162**, 1090-1100 (2015).
590 15. W. Bu *et al.*, Immunization with Components of the Viral Fusion Apparatus Elicits
591 Antibodies That Neutralize Epstein-Barr Virus in B Cells and Epithelial Cells. *Immunity*
592 **50**, 1305-1316 e1306 (2019).
593 16. T. Vesikari, S. Pepin, I. Kusters, A. Hoffenbach, M. Denis, Assessment of squalene
594 adjuvanted and non-adjuvanted vaccines against pandemic H1N1 influenza in children 6
595 months to 17 years of age. *Hum Vaccin Immunother* **8**, 1283-1292 (2012).
596 17. A. Carville, K. G. Mansfield, Comparative pathobiology of macaque
597 lymphocryptoviruses. *Comp Med* **58**, 57-67 (2008).
598 18. S. Fujiwara, K. Imadome, M. Takei, Modeling EBV infection and pathogenesis in new-
599 generation humanized mice. *Exp Mol Med* **47**, e135 (2015).

19. S. Fujiwara, G. Matsuda, K. Imadome, Humanized mouse models of epstein-barr virus infection and associated diseases. *Pathogens* **2**, 153-176 (2013).
20. M. Islas-Ohlmayer *et al.*, Experimental infection of NOD/SCID mice reconstituted with human CD34+ cells with Epstein-Barr virus. *J Virol* **78**, 13891-13900 (2004).
21. M. Yajima *et al.*, A new humanized mouse model of Epstein-Barr virus infection that reproduces persistent infection, lymphoproliferative disorder, and cell-mediated and humoral immune responses. *J Infect Dis* **198**, 673-682 (2008).
22. G. M. Escalante *et al.*, A Pentavalent Epstein-Barr Virus-Like Particle Vaccine Elicits High Titers of Neutralizing Antibodies against Epstein-Barr Virus Infection in Immunized Rabbits. *Vaccines (Basel)* **8**, (2020).
23. C. Cox *et al.*, Immunization of common marmosets with Epstein-Barr virus (EBV) envelope glycoprotein gp340: effect on viral shedding following EBV challenge. *J Med Virol* **55**, 255-261 (1998).
24. G. Khan, W. Ahmed, P. S. Philip, M. H. Ali, A. Adem, Healthy rabbits are susceptible to Epstein-Barr virus infection and infected cells proliferate in immunosuppressed animals. *Virol J* **12**, 28 (2015).
25. D. Espinosa *et al.*, Passive Transfer of Immune Sera Induced by a Zika Virus-Like Particle Vaccine Protects AG129 Mice Against Lethal Zika Virus Challenge. *EBioMedicine* **27**, 61-70 (2018).
26. M. K. Howard *et al.*, H5N1 whole-virus vaccine induces neutralizing antibodies in humans which are protective in a mouse passive transfer model. *PLoS One* **6**, e23791 (2011).
27. T. F. Rogers *et al.*, Isolation of potent SARS-CoV-2 neutralizing antibodies and protection from disease in a small animal model. *Science* **369**, 956-963 (2020).
28. C. Munz, Immune Control and Vaccination against the Epstein-Barr Virus in Humanized Mice. *Vaccines (Basel)* **7**, (2019).
29. W. Kabsch, Integration, scaling, space-group assignment and post-refinement. *Acta Crystallogr D Biol Crystallogr* **66**, 133-144 (2010).
30. W. Kabsch, Xds. *Acta Crystallogr D Biol Crystallogr* **66**, 125-132 (2010).
31. A. J. McCoy, Solving structures of protein complexes by molecular replacement with Phaser. *Acta Crystallogr D Biol Crystallogr* **63**, 32-41 (2007).
32. A. J. McCoy *et al.*, Phaser crystallographic software. *J Appl Crystallogr* **40**, 658-674 (2007).
33. P. Emsley, B. Lohkamp, W. G. Scott, K. Cowtan, Features and development of Coot. *Acta Crystallogr D Biol Crystallogr* **66**, 486-501 (2010).
34. P. D. Adams *et al.*, PHENIX: a comprehensive Python-based system for macromolecular structure solution. *Acta Crystallogr D Biol Crystallogr* **66**, 213-221 (2010).
35. A. E. Coghill *et al.*, High Levels of Antibody that Neutralize B-cell Infection of Epstein-Barr Virus and that Bind EBV gp350 Are Associated with a Lower Risk of Nasopharyngeal Carcinoma. *Clin Cancer Res* **22**, 3451-3457 (2016).
36. J. Sashihara, P. D. Burbelo, B. Savoldo, T. C. Pierson, J. I. Cohen, Human antibody titers to Epstein-Barr Virus (EBV) gp350 correlate with neutralization of infectivity better than antibody titers to EBV gp42 using a rapid flow cytometry-based EBV neutralization assay. *Virology* **391**, 249-256 (2009).

644 37. M. Gupta, S. Mahanty, M. Bray, R. Ahmed, P. E. Rollin, Passive transfer of antibodies
645 protects immunocompetent and imunodeficient mice against lethal Ebola virus infection
646 without complete inhibition of viral replication. *J Virol* **75**, 4649-4654 (2001).
647 38. J. Maamary, T. T. Wang, G. S. Tan, P. Palese, J. V. Ravetch, Increasing the breadth and
648 potency of response to the seasonal influenza virus vaccine by immune complex
649 immunization. *Proc Natl Acad Sci U S A* **114**, 10172-10177 (2017).
650 39. T. Strowig *et al.*, Priming of protective T cell responses against virus-induced tumors in
651 mice with human immune system components. *J Exp Med* **206**, 1423-1434 (2009).
652 40. E. F. Pettersen *et al.*, UCSF Chimera--a visualization system for exploratory research and
653 analysis. *J Comput Chem* **25**, 1605-1612 (2004).

654

655

656

657

658

659

660

661

662

663

A


B

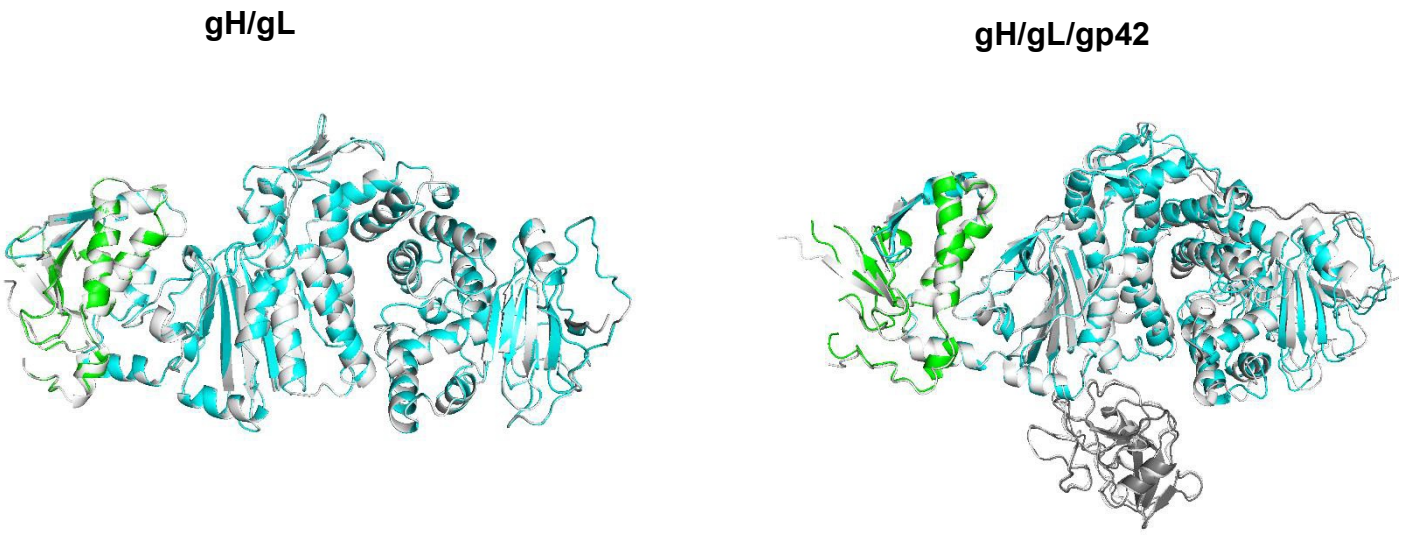


C

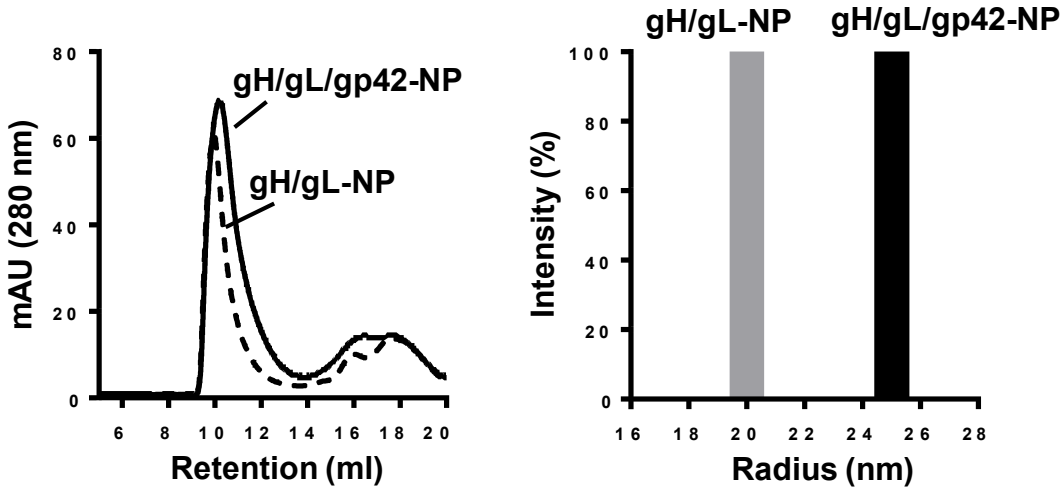


D

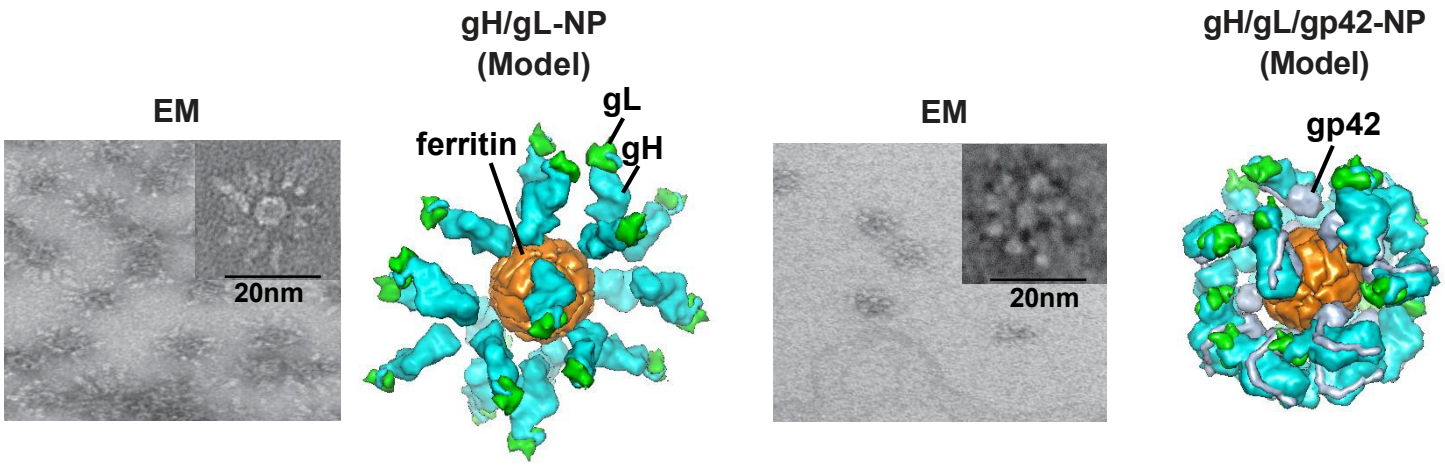

Figure 2

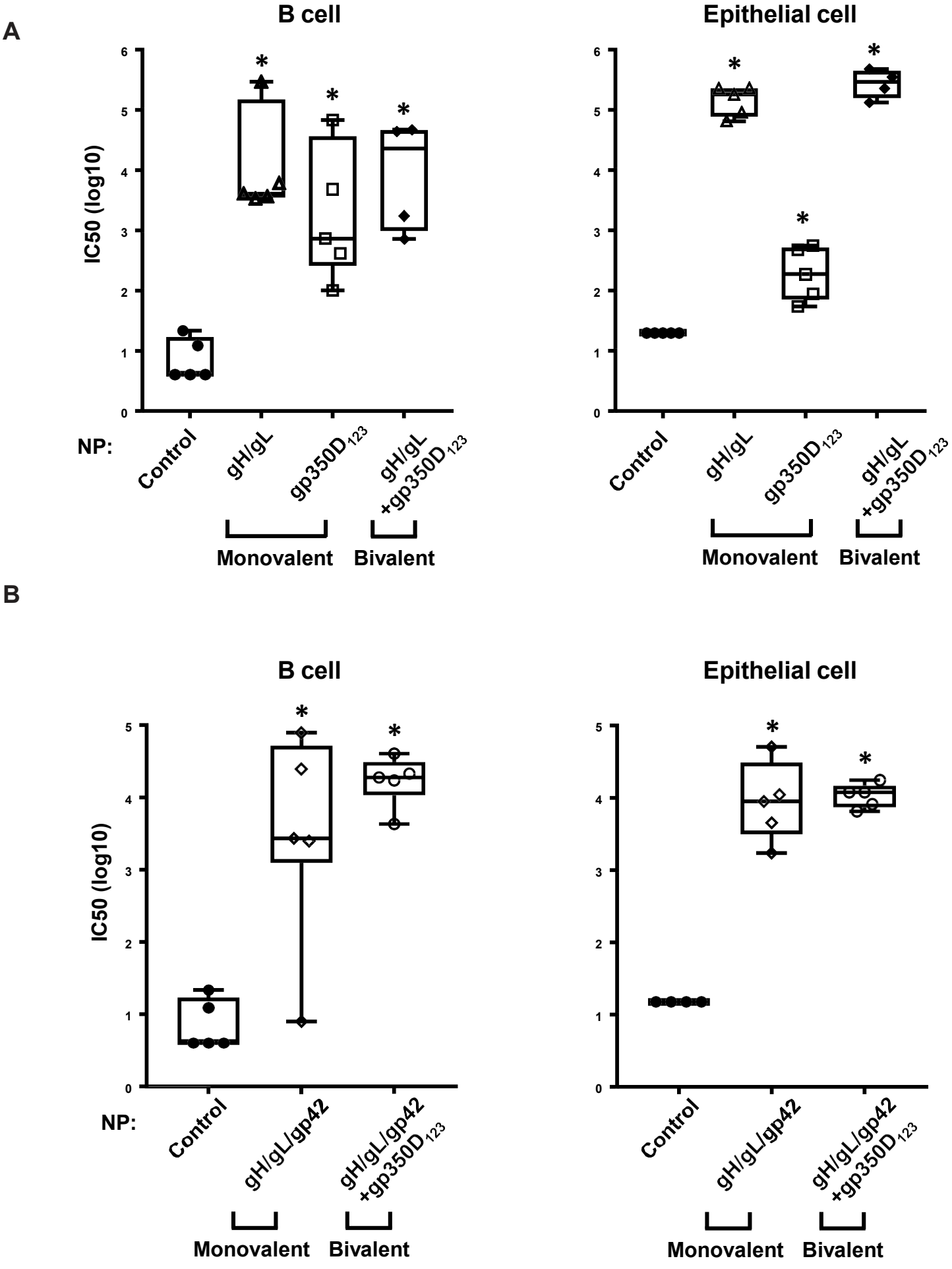

Figure 3

A

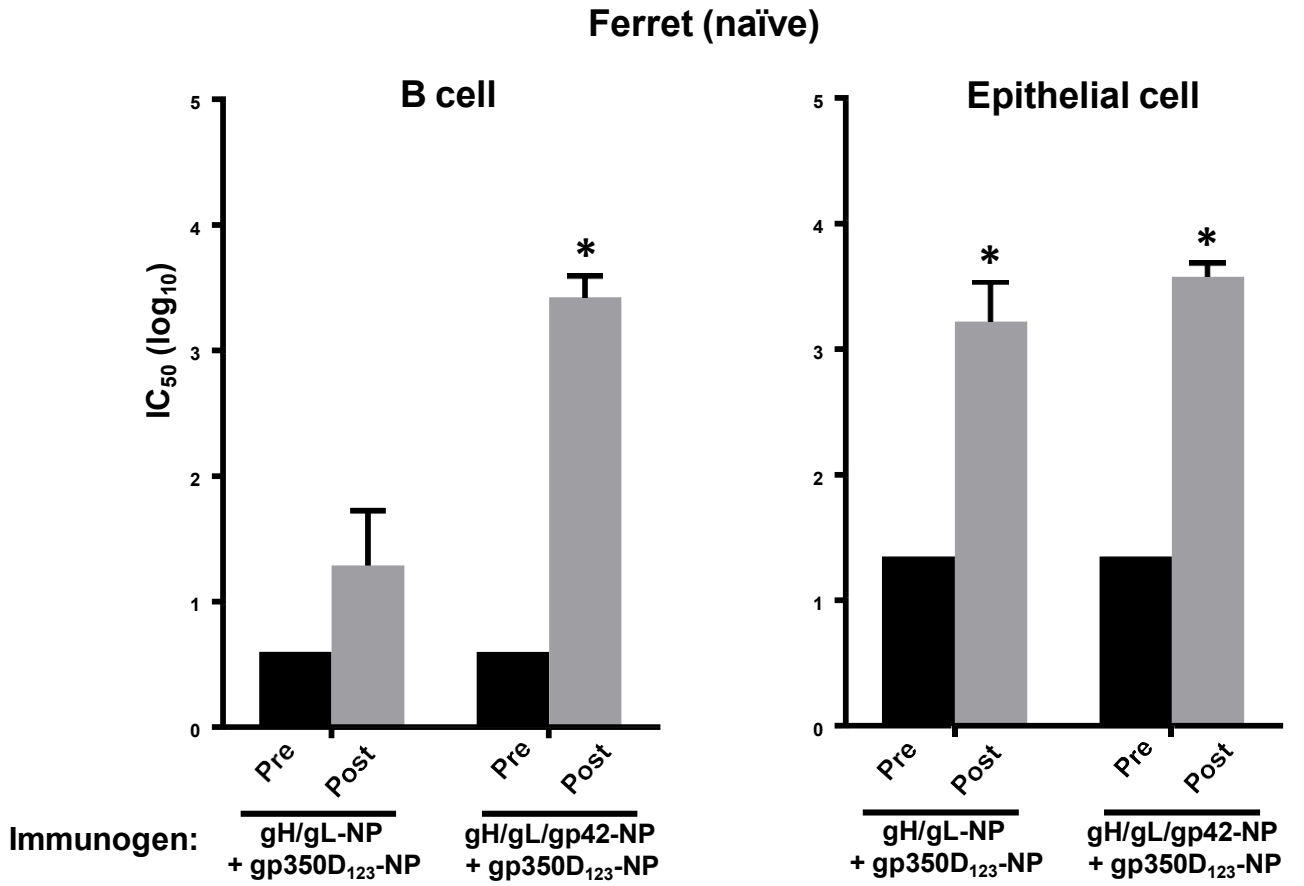


B

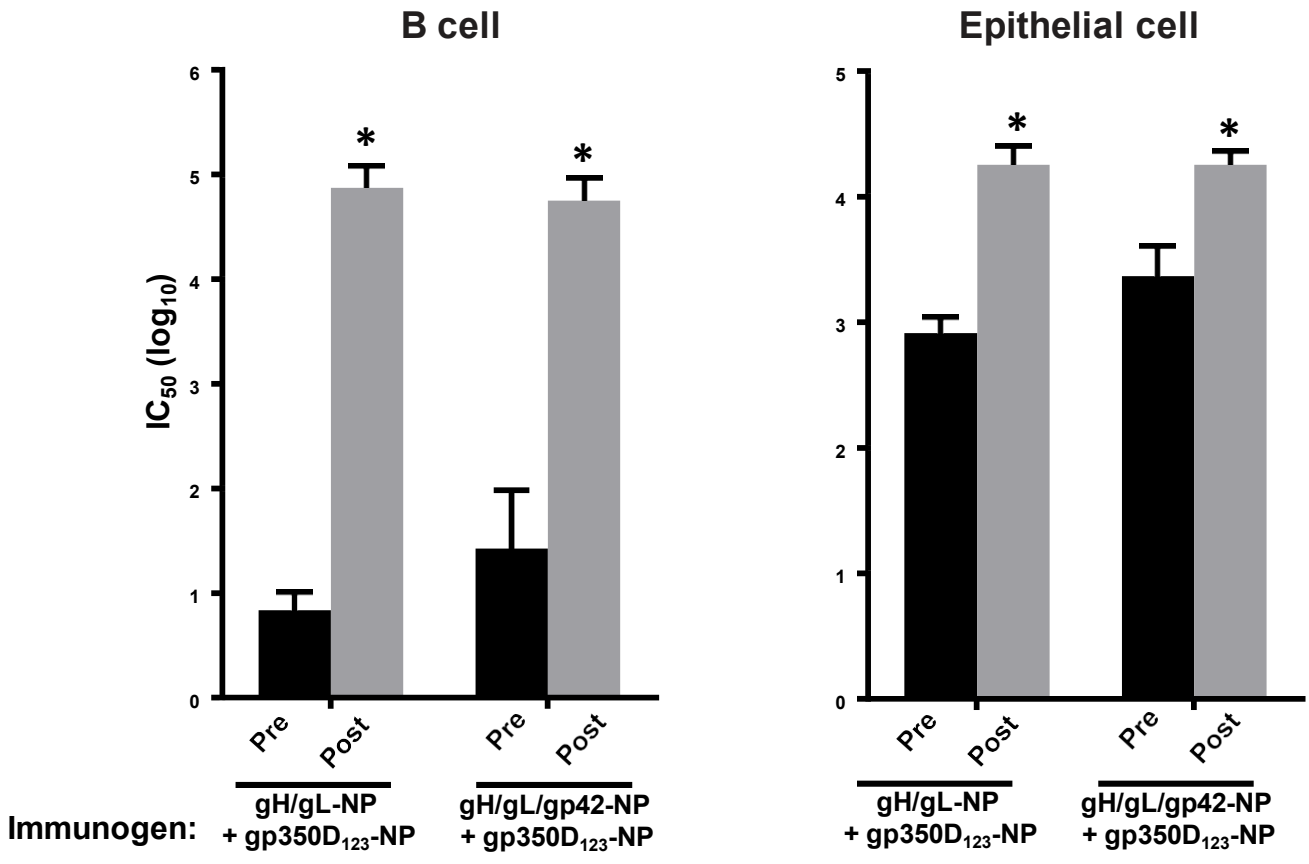

# Figure 4

**A**

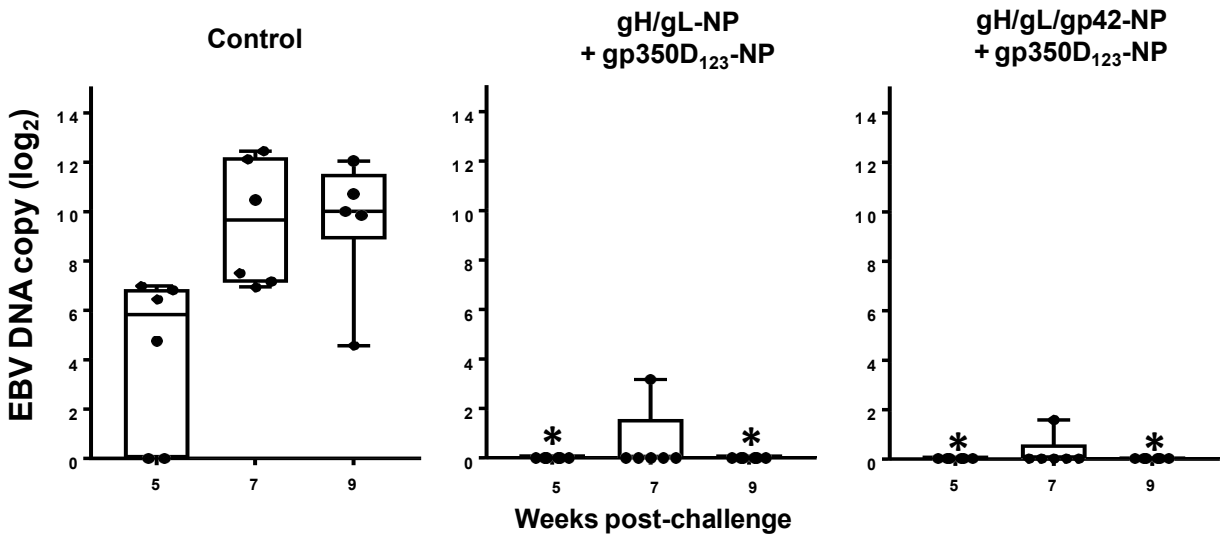


**B**

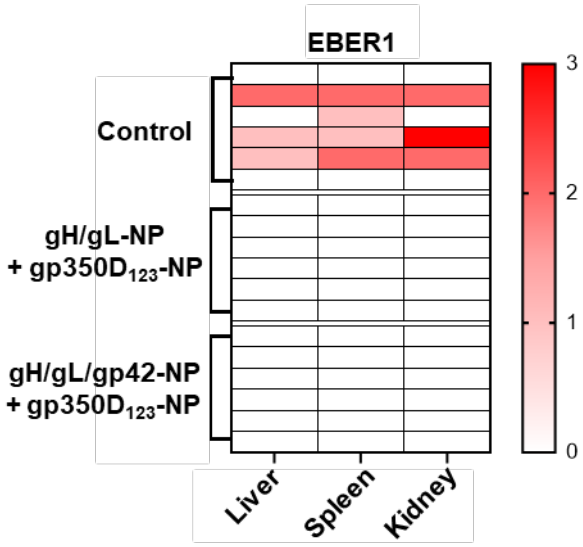

Figure 5

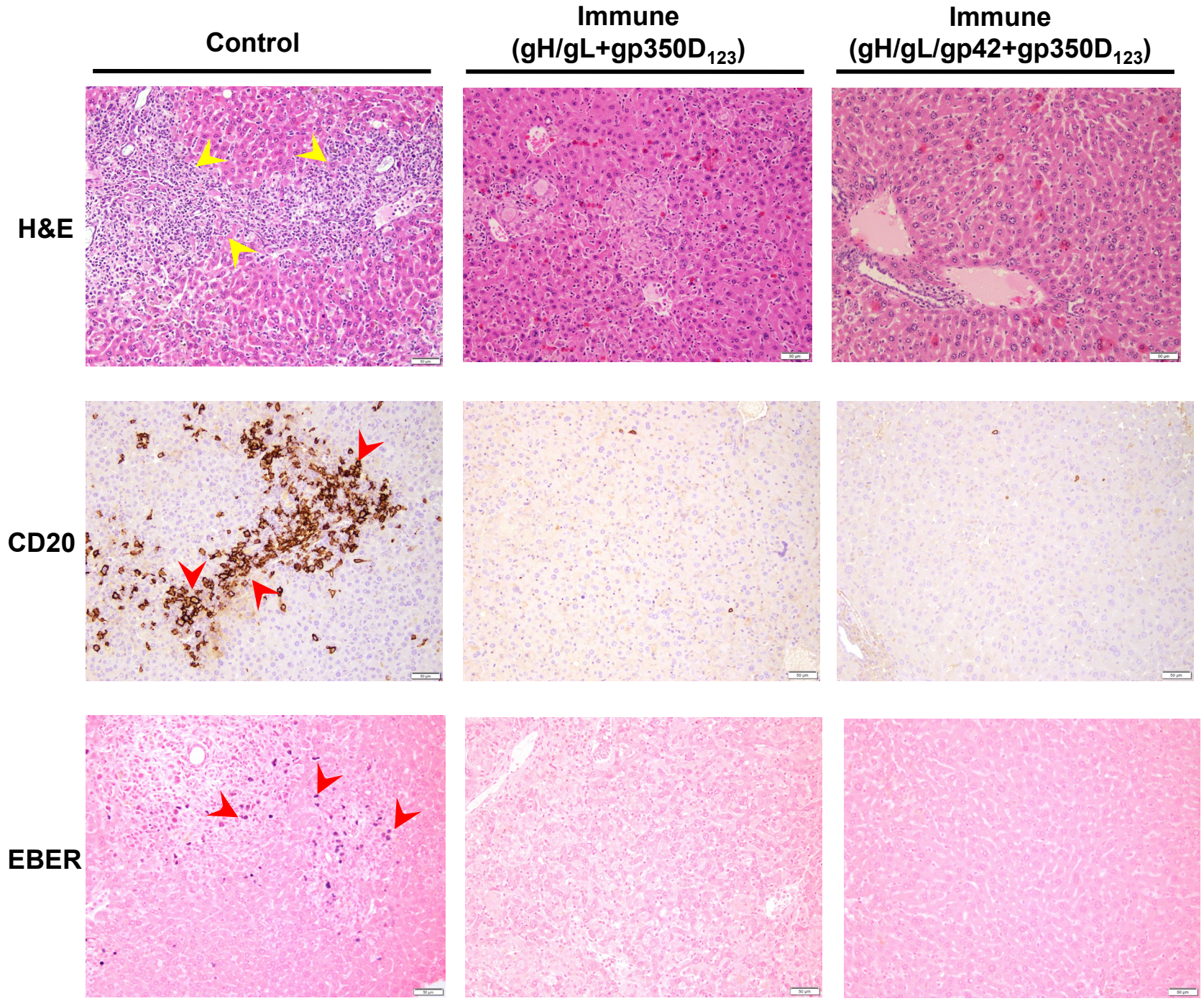
Control
Immune (gH/gL+gp350D123)
Immune (gH/gL/gp42+gp350D123)
H&E
CD20
EBER

# Supplemental Figure 1

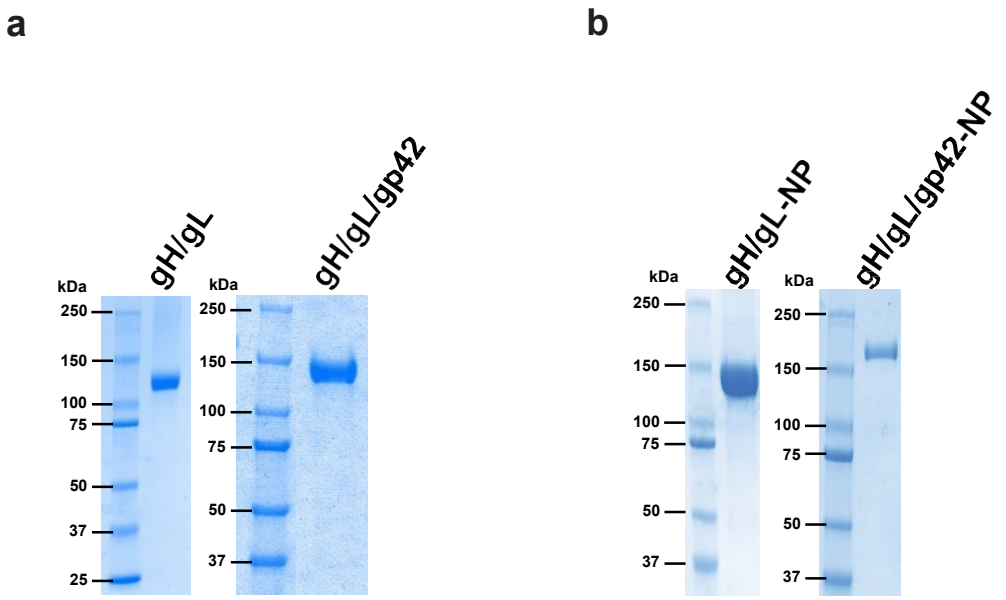

**Supplemental Figure 2**

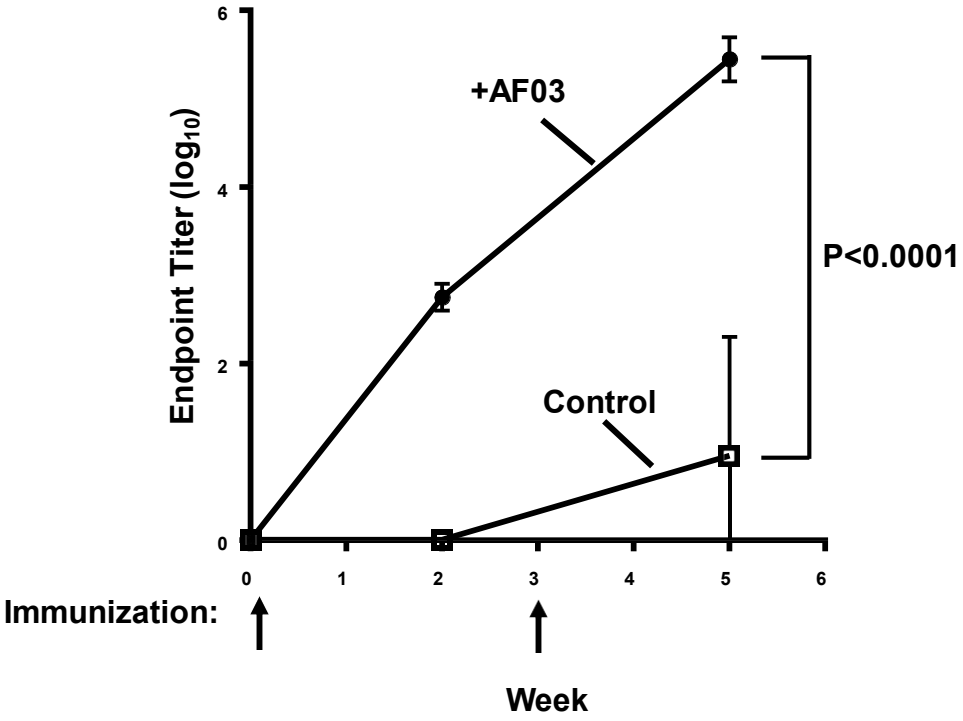

# Supplemental Figure 3

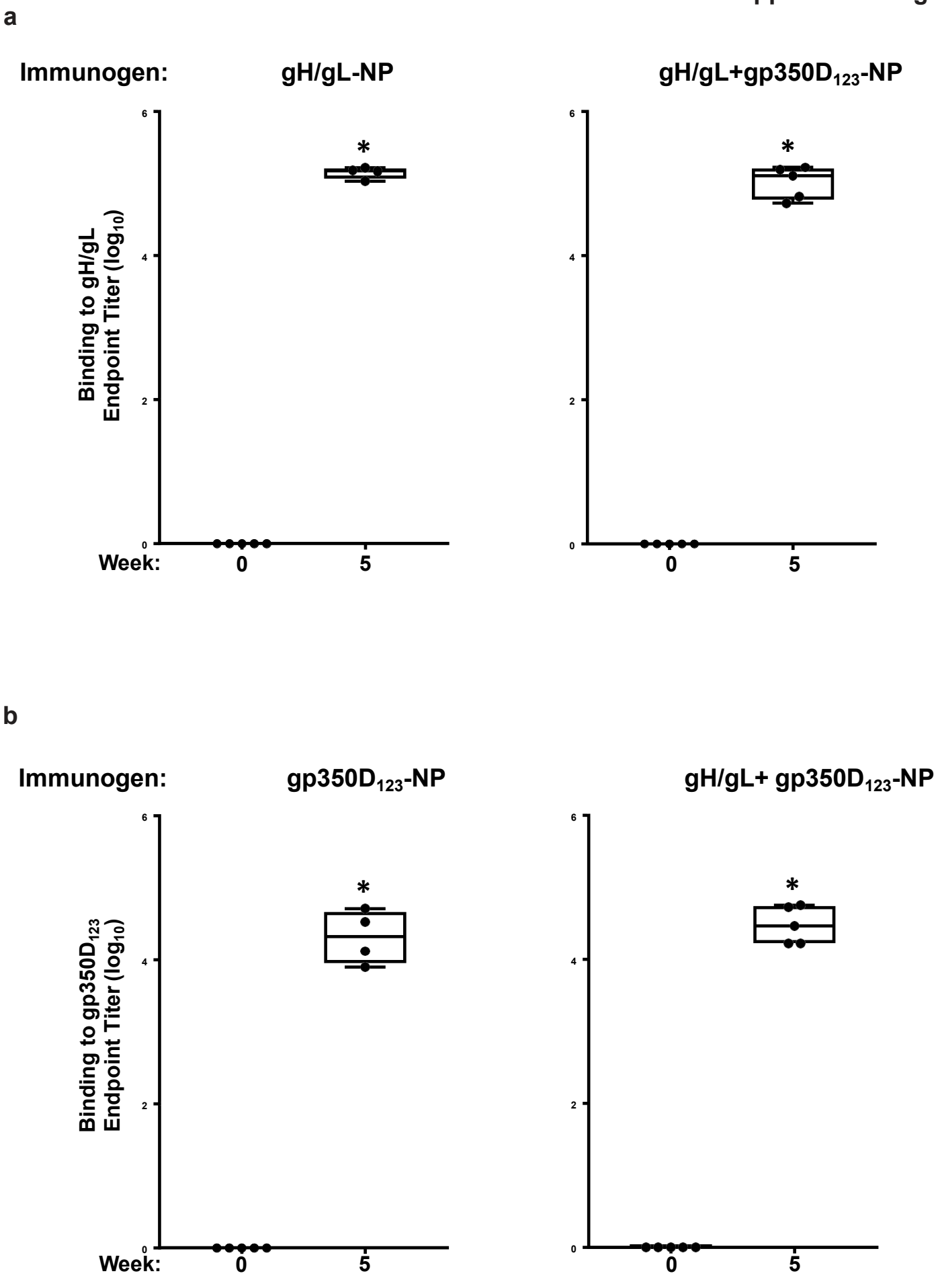

# Supplemental Figure 4

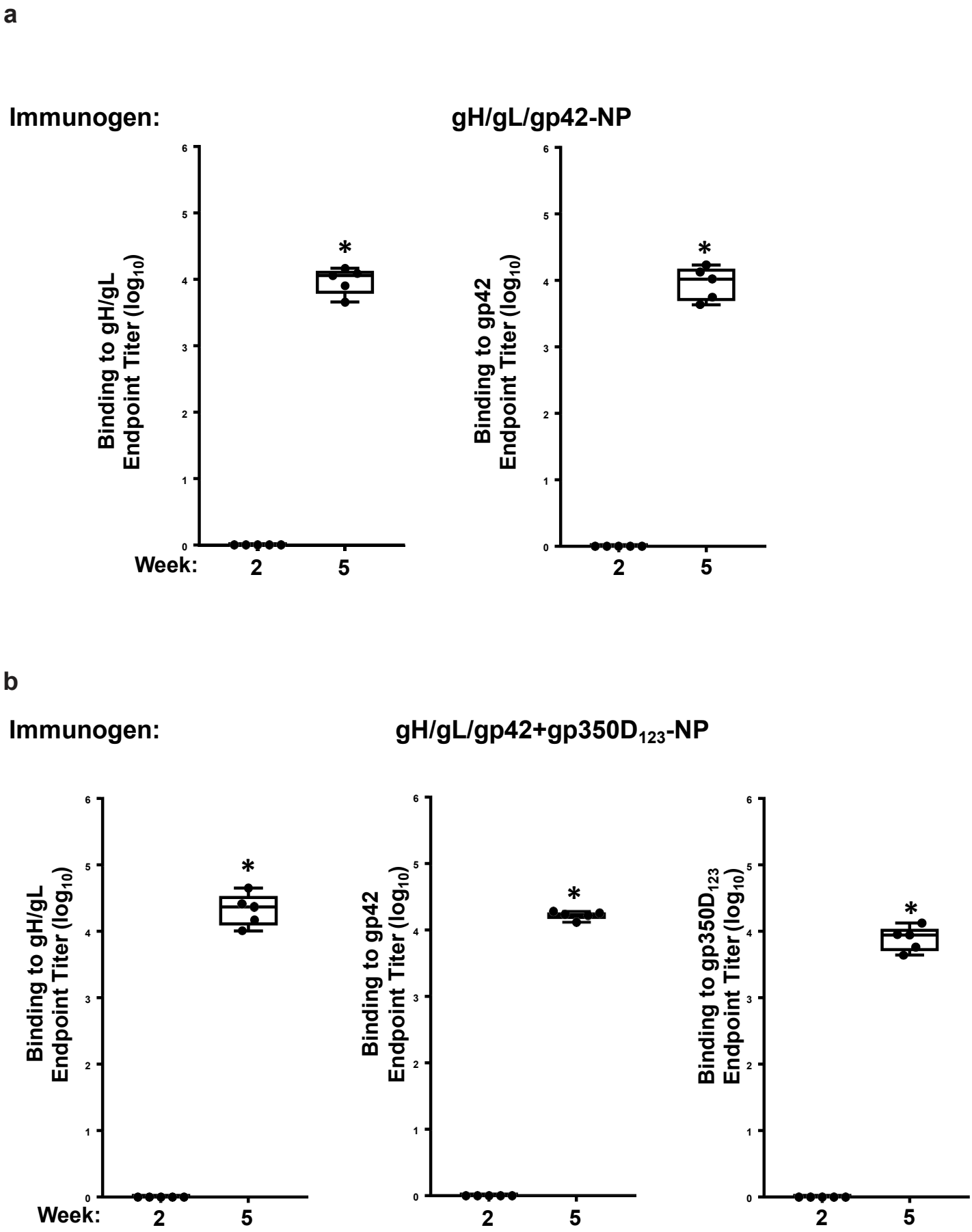

**Supplemental Figure 5**

**Immunogen: gH/gL-NP + gp350D$_{123}$-NP**

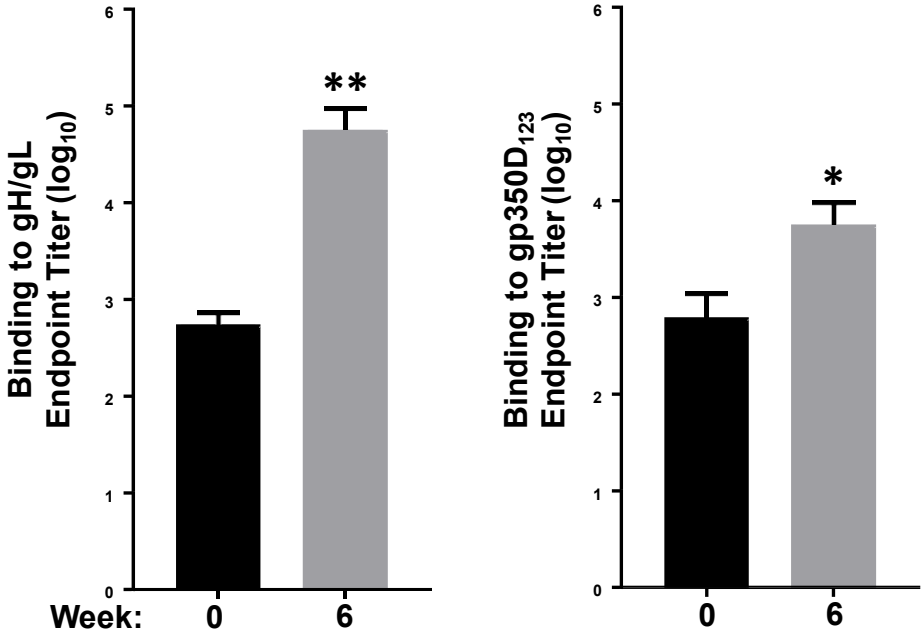


**Immunogen: gH/gL/gp42-NP + gp350D$_{123}$-NP**

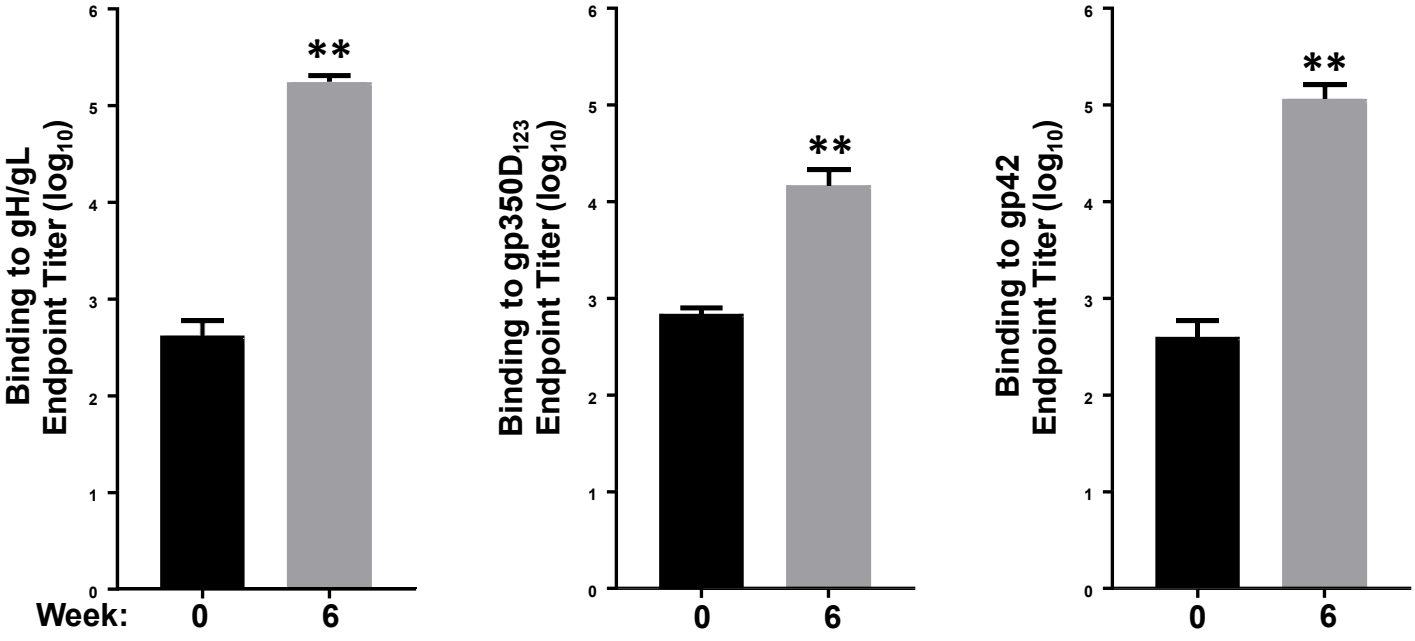

**Supplemental Figure 6**

**Immunogen: gH/gL-NP + gp350D$_{123}$-NP**

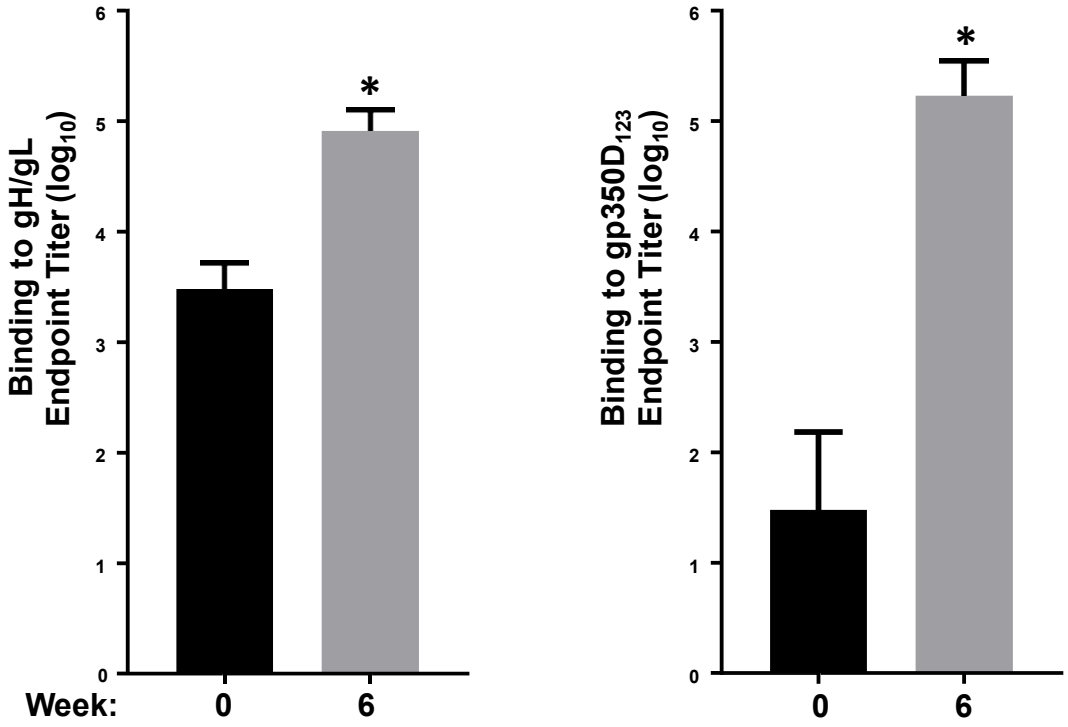


**Immunogen: gH/gL/gp42-NP + gp350D$_{123}$-NP**

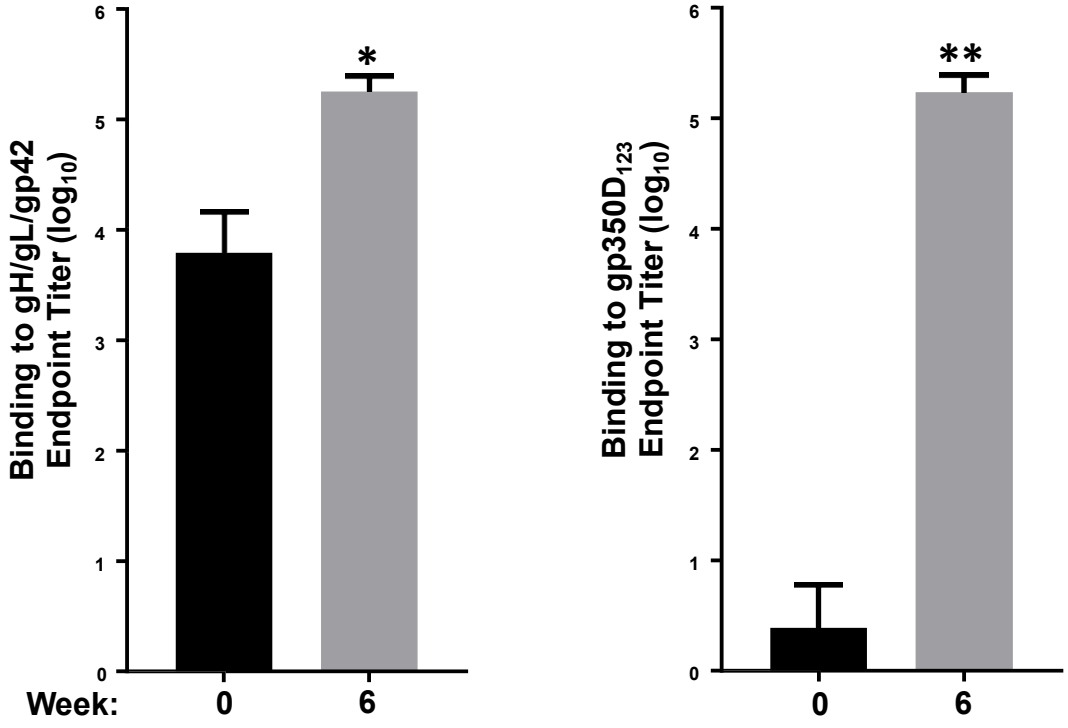

Supplemental Figure 7

a

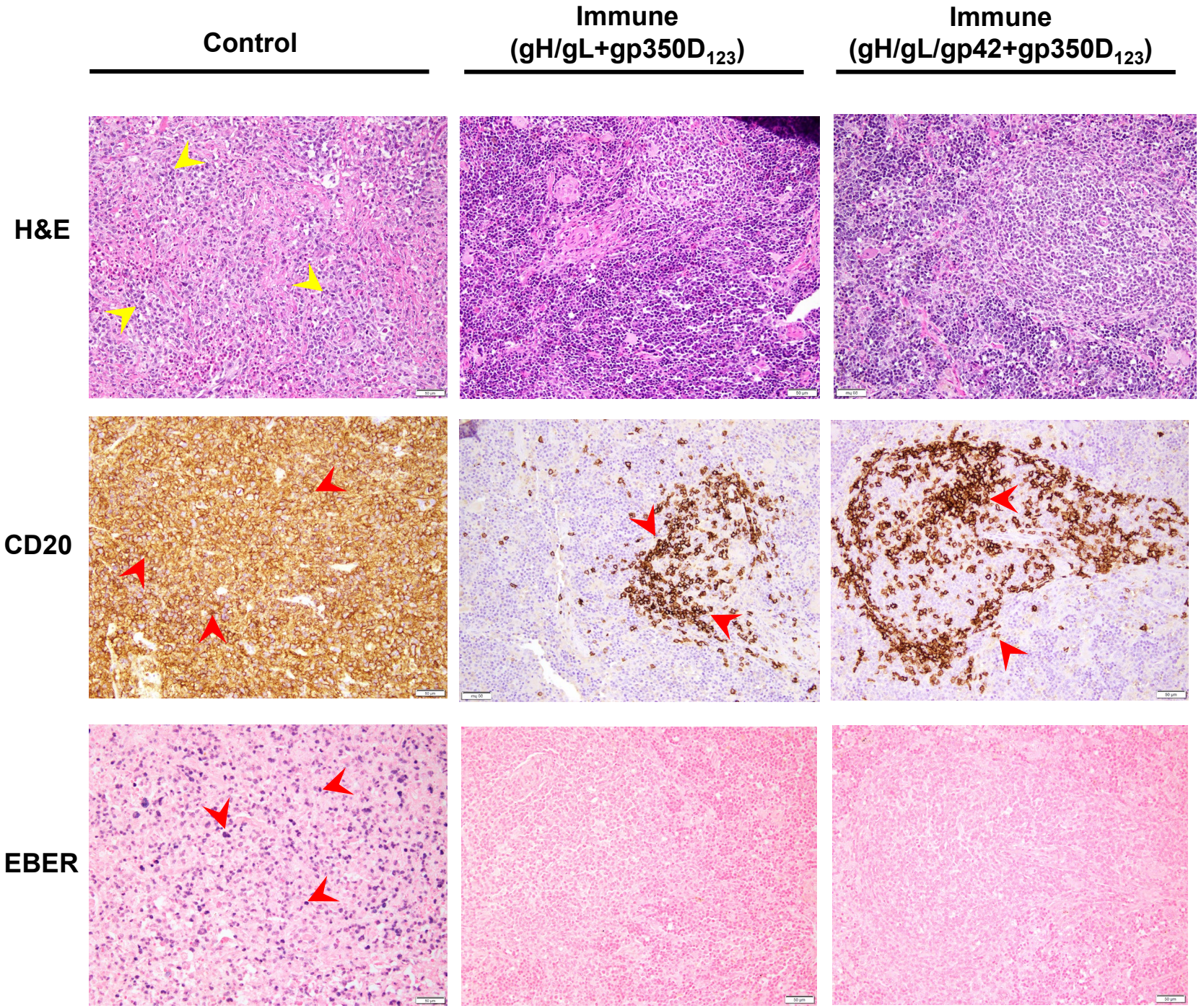

b

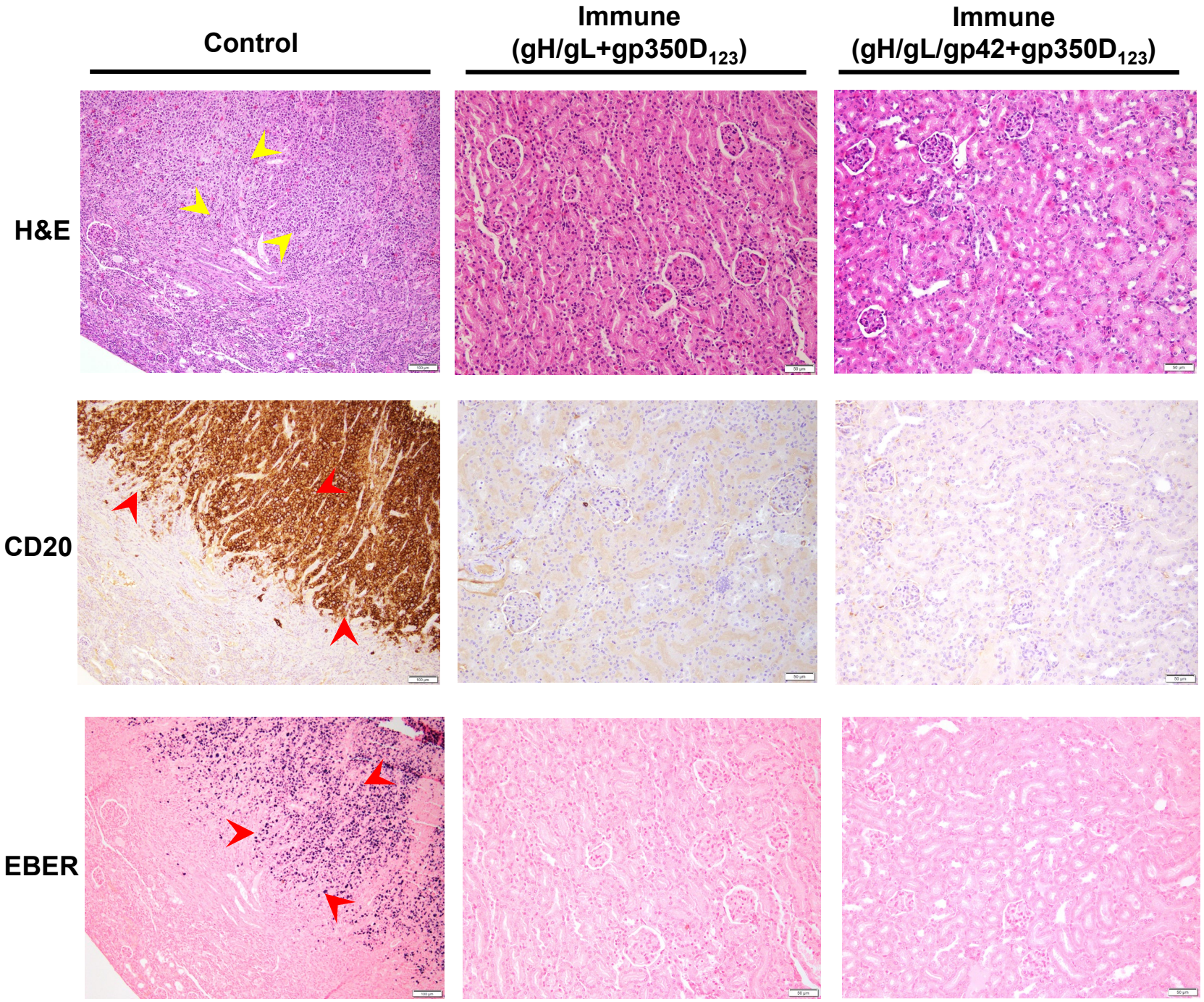
Control
Immune (gH/gL+gp350D123)
Immune (gH/gL/gp42+gp350D123)
H&E
CD20
EBER

**Supplemental Fig. 8**